

1 **Intra-annual variability of the Western Mediterranean Oscillation (WeMO)**
2 **and occurrence of extreme torrential precipitation in Catalonia (NE Iberia)**

3 Joan A. Lopez-Bustins (1), L. Arbiol-Roca (1), J. Martin-Vide (1), A. Barrera-
4 Escoda (2) and M. Prohom (1,2)

5 (1) Climatology Group, Department of Geography, University of Barcelona
6 (UB), Barcelona, Spain.

7 (2) Department of Climatology, Meteorological Service of Catalonia,
8 Barcelona, Spain.

9
10 **Abstract**

11 In previous studies the Western Mediterranean Oscillation index (WeMOi) at daily
12 resolution has proven to constitute an effective tool for analysing the occurrence of
13 episodes of torrential precipitation over eastern Spain. The Western Mediterranean
14 region is therefore a very sensitive area, since climate change can enhance these
15 weather extremes. In the present study we created a catalogue of the extreme
16 torrential episodes (≥ 200 mm in 24 hours) that took place in Catalonia (NE Iberia)
17 during the 1951-2016 study period (66 years). We computed daily WeMOi values
18 and constructed WeMOi calendars. Our principal results reveal the occurrence of
19 50 episodes (0.8 cases per year), mainly concentrated in the autumn. We
20 confirmed a threshold of WeMOi ≤ -2 to define an extreme negative WeMO phase
21 at daily resolution. Most of the 50 episodes (60%) in the study area occurred on
22 days presenting an extreme negative WeMOi value. Specifically, the most negative
23 WeMOi values are detected in autumn, during the second 10-day period of October
24 (11th-20th), coinciding with the highest frequency of extreme torrential events. On
25 comparing the subperiods, we observed a statistically significant decrease in
26 WeMOi values in all months, particularly in late October, and in November and
27 December. No changes in the frequency of these extreme torrential episodes were
28 observed between both subperiods. In contrast, a displacement of the extreme
29 torrential episodes is detected from early to late autumn; this can be related to a
30 statistically significant warming of sea temperature.

31 **Keywords**

32 Mediterranean, sea temperature, teleconnection indices, torrential precipitation,
33 WeMO.

34 1. Introduction

35 The Mediterranean seasonal precipitation regime is characterised by rainy
36 winters and dry summers, linked to the westerly atmospheric circulation in winter
37 and to the subtropical anticyclone belt in summer. Nevertheless, in some regions
38 of the Mediterranean basin, the seasonal precipitation regime differs from the
39 typically Mediterranean one; for example, most of eastern Iberia (Spain) displays
40 a seasonal precipitation maximum in autumn, and a secondary one in spring (De
41 Luis *et al.*, 2010; González-Hidalgo *et al.*, 2011). This bimodal precipitation
42 pattern is recorded in few regions of the world. It only occurs over approximately
43 7% of the global land surface, and is commonly associated with locations within
44 the tropics (Knoben *et al.*, 2019). This bimodal behaviour in eastern Spain is
45 mainly due to the physical geographic complexity of the Iberian Peninsula, which
46 comprises several mountain ranges, all of which present different slope
47 orientations. Furthermore, the Mediterranean Sea is practically cut off from other
48 water bodies, which favours a higher sea surface temperature (SST) than in the
49 Atlantic at the same latitude, especially in summer and autumn (Pastor *et al.*,
50 2015). This contributes to the development of high vertical gradients of air
51 temperature in some months over the Mediterranean basin (Estrela *et al.*, 2008;
52 Pérez-Zanón *et al.*, 2018). These physical geographical factors give rise to a high
53 concentration of daily precipitation in the Mediterranean basin, i.e. torrential
54 precipitation events, above all in the Western Mediterranean (Beguería *et al.*,
55 2011; Cortesi *et al.*, 2012; Caloiero *et al.*, 2019); all this reveals the need for water
56 management in Spain to be based upon precipitation variability rather than on
57 the precipitation mean (Lopez-Bustins, 2018). Heavy precipitation in the Western
58 Mediterranean is mainly centred in eastern Spain, the south of France and the
59 region of Liguria (NW Italy) (Peñarrocha *et al.*, 2002). These torrential events can
60 cause dangerous floods and can have serious social and economic
61 consequences, even human casualties, in the Mediterranean regions, e.g. in
62 eastern Spain (Olcina *et al.*, 2016; Kreibich *et al.*, 2017; Nakamura and Llasat,
63 2017; Martin-Vide and Llasat, 2018) and in southern Spain (Gil-Guirado *et al.*,
64 2019; Naranjo-Fernández *et al.*, 2020). Climatological studies on torrential
65 precipitation frequency and intensity are therefore relevant with regard to
66 improving emergency plans and mitigating flood damage. Extreme precipitation

67 is expected to increase with global warming as a result of a greater atmospheric
68 water content (Papalexiou and Montanari, 2019); for instance, extreme peak river
69 flows are predicted to increase in Southern Europe during the current century
70 (Alfieri *et al.*, 2015), and the frequency of heavy precipitation events is projected
71 to be higher for the 2011-2050 period (Barrera-Escoda *et al.*, 2014).

72 Previous studies have associated extreme daily precipitation events in Spain with
73 synoptic patterns (Martin-Vide *et al.*, 2008; Peña *et al.*, 2015); these studies have
74 addressed several different tropospheric levels (Romero *et al.*, 1999; Merino *et al.*
75 *et al.*, 2016; Pérez-Zanón *et al.*, 2018). Furthermore, many studies have also
76 statistically correlated several teleconnection indices (El Niño Southern
77 Oscillation, North Atlantic Oscillation, Arctic Oscillation, Mediterranean
78 Oscillation, Western Mediterranean Oscillation, etc.) with precipitation series for
79 the Iberian Peninsula at different timescales (Rodó *et al.*, 1997; Rodríguez-
80 Puebla *et al.*, 2001; Trigo *et al.*, 2004; Lopez-Bustins *et al.*, 2008; González-
81 Hidalgo *et al.*, 2009; Ríos-Cornejo *et al.*, 2015a; Merino *et al.*, 2016). Among
82 these indices, the Western Mediterranean Oscillation (WeMO) was found to be
83 the index most statistically and significantly correlated with annual, monthly and
84 daily precipitation on the littoral fringe of eastern Spain (Martin-Vide and Lopez-
85 Bustins, 2006; González-Hidalgo *et al.*, 2009). The daily timescale of the WeMO
86 index (WeMOi) could constitute a potential tool for analysing the frequency of
87 torrential events in some regions of the Western Mediterranean basin.

88 Most torrential events in the Mediterranean region present a cyclonic centre at
89 surface level (Jansà *et al.*, 1996; Rigo and Llasat, 2003). These cyclonic centres,
90 which are mainly mesoscale lows, can contribute to the structure of low-level
91 flows and therefore to the creation or intensification of a low-level warm and wet
92 current that can feed and sustain convection in favourable environmental
93 conditions (Jansà and Genovés, 2000; Jansà *et al.*, 2000). Furthermore, the
94 Mediterranean Sea moistens and warms the low level of the atmosphere.
95 Consequently, the southerly to easterly flow that prevails before and during
96 torrential events in the Western Mediterranean transports the air under
97 conditional instability toward the coasts, where convection is often triggered by
98 an interaction between the flow and the orography. Studies based upon
99 mesoscale modelling, such as the research conducted by Lebeaupin *et al.*

100 (2006), show that an increase (or a decrease) in SST by several degrees
101 intensifies (or weakens) convection. In addition, the presence of a cut-off low in
102 the upper troposphere might be playing a significant role in the occurrence of
103 heavy precipitation, creating a cyclonic circulation in the lower troposphere, thus
104 enabling Atlantic air to be carried over the Mediterranean Sea. This warm and
105 very wet air in the lower layers impinges on the coastal mountains ranges and
106 the forced ascent is sufficient to trigger potential instability. This meteorological
107 configuration is accounted for the negative phase of the WeMO, which defines a
108 synoptic pattern prone to producing torrential precipitation and floods on the
109 Eastern Iberian coast. Daily precipitation amounts over 200 mm are not unusual
110 in such cases, particularly in eastern Spain, where many catastrophic floods are
111 related to the presence of a cut-off low (Llasat, 2009). Thus, these catastrophic
112 floods in the Northwestern Mediterranean basin are generally of synoptic origin
113 and are defined by the negative phase of the WeMO and enhanced by certain
114 mesoscale factors (Gilabert and Llasat, 2018).

115 The present study provides an exhaustive inventory of the most intense daily
116 precipitation events in Catalonia (NE Iberia) over the last few decades (1951-
117 2016) in order to provide a better understanding of their temporal distribution.
118 Moreover, we will analyse changes in frequency according to subperiods, since
119 the Western Mediterranean basin constitutes a global warming hotspot, where a
120 decrease in mean annual precipitation is expected for the following decades,
121 particularly in summer, together with a potential rise in storm-related precipitation
122 and drought duration (Christensen *et al.*, 2013; Barrera-Escoda *et al.*, 2014;
123 Cramer *et al.*, 2018; Greve *et al.*, 2018). The main aim of our study involves
124 creating a catalogue of extreme torrential events in Catalonia in order to establish
125 a period of high potential torrentiality in the area analysed at daily resolution. Most
126 studies delimit the wet season of a region within one or several months (Kottek
127 *et al.*, 2006), and do not employ a smaller timescale than the monthly one.
128 Consequently, the present research attempts to use a more accurate timescale
129 than the monthly one in order to determine the period with the highest
130 accumulation of heavy precipitation episodes according to fortnights and 10-day
131 periods. The intra-annual variability of the daily WeMOi values may help to
132 establish the period with the highest propensity for torrential events in Catalonia.

133 Additionally, we analyse SST in order to establish a sea-atmosphere interaction
134 to explain WeMOi values and changes in the frequency of events. Seawater
135 constitutes an energy store, i.e. recharge areas, which can influence water
136 vapour content and can intensify precipitation episodes (Pastor *et al.*, 2018;
137 Iizuka and Nakamura, 2019) by means of a sea-atmosphere moisture exchange.
138 Furthermore, a significant release of latent heat occurs during atmospheric
139 convection over a warm sea like the Mediterranean at the end of summer and the
140 beginning of autumn (Pastor *et al.*, 2015).

141 In section 2, we describe the main orographic and pluviometric features of the study
142 area. The data and methods followed to calculate daily WeMOi values and construct
143 the WeMOi calendar are explained in section 3. In section 4, the results of the intra-
144 annual variability of torrential episodes, WeMOi values and sea temperature trends
145 are analysed and discussed. Finally, in section 4 we derive the conclusions.

146

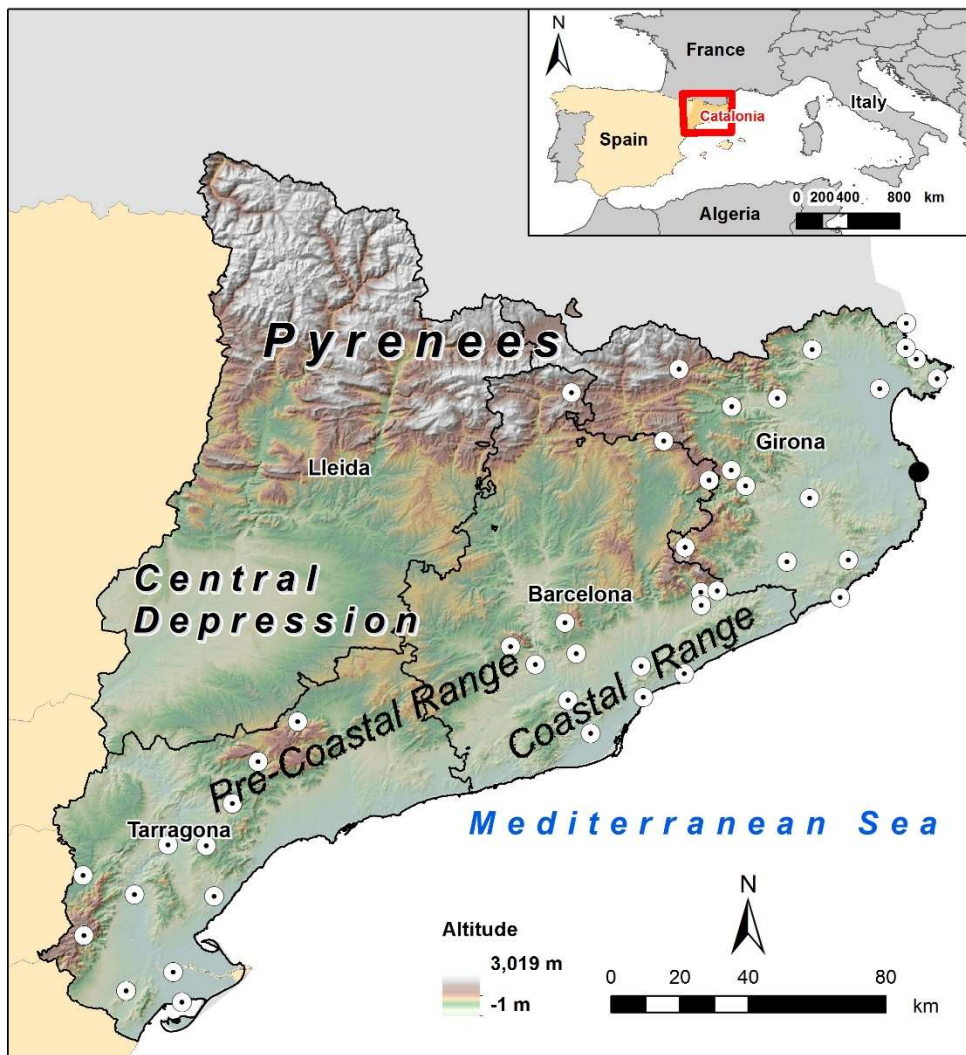
147 **2. Study area**

148 Catalonia covers an area of 32,100 km² in northeast Spain; it is physically separated
149 from France by the Pyrenees (Figure 1). Altitude ranges from 0 (littoral) to 3,100
150 (northwestern Pyrenees) m.a.s.l. The Coastal and Pre-Coastal ranges, with an
151 altitude ranging from 500 to 1,700 m.a.s.l., present a SW-NE orientation. On the
152 western border, the Central Depression is approximately 200-300 m.a.s.l.,
153 constituting the driest part of the study area (350 mm annual mean precipitation)
154 (Figure 2a). The wettest part of Catalonia is located in the Pyrenees, with an annual
155 mean precipitation over 1,200 mm. In general terms, southern Lleida and Barcelona,
156 as well as almost the entire province of Tarragona, make up the dry part of Catalonia
157 (<700 mm). The rainy part of Catalonia (≥ 700 mm) comprises the province of Girona
158 and the northern halves of the provinces of Lleida and Barcelona.

159 Catalonia's complex orography, as well as the fact that it comes under the influence
160 of the Atlantic Ocean and the Mediterranean Sea, endow it with a highly
161 heterogeneous spatial distribution of seasonal precipitation regimes throughout the
162 study area. Using 70 monthly precipitation series (1951-2016) homogenized and
163 provided by the Meteorological Service of Catalonia (SMC, 2017), we ascertained
164 that, of the total of 24 possible permutations between winter, spring, summer and

165 autumn as dominant and subdominant precipitation seasons, 7 of these are detected
166 in Catalonia (Figure 2b) (Martin-Vide and Raso-Nadal, 2008). A clear predominance
167 of autumn precipitation can be observed, followed by spring precipitation, especially
168 in the coastal zone. The driest season on the coast is summer; however, the driest
169 time of year inland is winter. Many areas of the Pyrenees, above all in the east,
170 exhibit their maxima in summer as a result of convective precipitation.

171

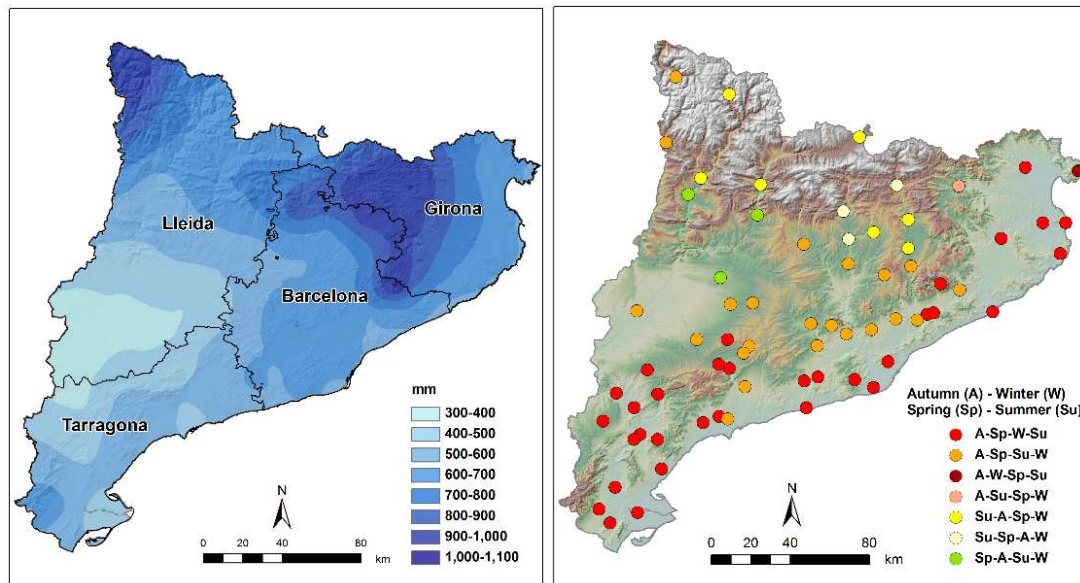


172

173 Figure 1. Location of Catalonia (NE Spain) within Europe, altitude and provinces.
174 The white dots indicate the 43 different weather stations that have recorded the
175 highest precipitation amount during an extreme torrential event at least once in
176 Catalonia during the 1951-2016 study period. The black dot indicates the location
177 of the sea temperature series. Base map provided by the Cartographic and
178 Geographical Institute of Catalonia.

(a)

(b)



180

181 Figure 2. (a) Annual mean precipitation (mm) and (b) seasonal precipitation
 182 regimes for 70 weather stations in Catalonia for the 1951-2016 study period.
 183 Data source: SMC (2017). Base map provided by the Cartographic and
 184 Geological Institute of Catalonia.

185

186 3. Data and methods

187 3.1. Selection of torrential events

188 Several studies have selected the torrential precipitation events in Spain based
 189 on the threshold of 100 mm in 24 h (Pérez-Cueva, 1994; Martin-Vide and Llasat,
 190 2000; Armengot, 2002; Riesco and Alcover, 2003; Martin-Vide *et al.*, 2008).
 191 Herein we chose the extreme torrential episodes (≥ 200 mm in 24 h) (Martin-Vide,
 192 2002; Lopez-Bustins *et al.*, 2016) that took place over Catalonia during the 1951-
 193 2016 study period (66 years). We consider the threshold of 200 mm in 24 h to
 194 present a natural risk in most cases, with significant consequences. Episodes
 195 involving ≥ 100 mm in 24 h are more frequent, but sometimes have no direct
 196 impact, or quite a negligible effect, because other factors are the main drivers of
 197 floods, e.g. precipitation duration (Jang, 2015), initial soil moisture conditions and
 198 hydrological parameters (Norbiato *et al.*, 2008; Martina *et al.*, 2009). Furthermore,
 199 the area affected by episodes of ≥ 100 mm in 24 h is sometimes local and is

200 therefore not easily associated with advective synoptic patterns (Gilabert and
201 Llasat, 2018).

202 In order to select the extreme torrential events, we considered all available
203 precipitation data sources in Catalonia (Meteorological Service of Catalonia,
204 Spanish National Meteorological Agency, Catalan Water Agency and Ebro
205 Hydrographic Confederation). Thus, 1,054 weather stations were identified
206 during 1951-2016, of which 749 were manually managed (71.1%) and provided
207 one register per day, at 7 h UTC. Until 1987 the manual weather stations had
208 constituted the only precipitation data source in Catalonia. The remaining 305
209 weather stations were automatic observatories, reporting hourly or semi-hourly
210 data depending on the network and period. The 1988-2016 period was covered
211 by both manual and automatic stations. We considered the pluviometric day as
212 7-7 UTC in both types of observatories in order to ensure a homogeneous
213 criterion when selecting episodes along the whole study period and analysing any
214 temporal changes in their frequency. We conducted an exhaustive spatial and
215 temporal verification of the extreme torrential episodes identified. We tested the
216 reliability of the events considering the daily precipitation recorded in
217 neighbouring stations and examining the original handwritten observation cards.
218 Furthermore, we rectified several episodes recorded by weather stations the day
219 after the pluviometric day, and we eliminated events derived from the
220 accumulation of precipitation for over one day.

221 The catalogue of extreme torrential events in Catalonia contains the following
222 columns: date, maximum precipitation in 24 h, location, province and daily
223 WeMOi value. Several observatories in Catalonia can occasionally register ≥ 200
224 mm in 24 h on one same date, but only the highest amount was taken into
225 account. Finally, we obtained 50 extreme torrential events for consideration in the
226 present study (Table 1). A total of 32 out of the 50 episodes (64%) have a decimal
227 place of 0, and 10 out of the 50 episodes (20%) present a decimal place of 5.
228 Most of these episodes were registered by manual weather stations prior to the
229 1990s. This is known as the rounding effect (Wergen *et al.*, 2012): a weather
230 observer rounds off the daily precipitation accumulation value during heavy
231 precipitation events. This effect has no influence on the results of the present
232 research.

Date	Max RR (mm)	Location	Province	WeMOi value
13 October 1986	430.0	Cadaqués	Girona	-2.22
11 April 2002	367.5	Darnius	Girona	-3.85
20 September 1971	308.0	Esparreguera	Barcelona	-1.75
20 September 1972	307.0	Sant Carles de la Ràpita	Tarragona	-1.58
09 October 1994	293.0	Cornudella de Montsant	Tarragona	-2.88
03 October 1987	291.0	Castelló d'Empúries	Girona	-1.96
22 September 1971	285.0	Cadaqués	Girona	-2.19
19 October 1977	276.0	Cadaqués	Girona	-2.80
21 September 1971	275.0	Santa Maria de Palautordera	Barcelona	-2.21
18 October 1977	271.8	Camprodon	Girona	-2.21
21 October 2000	270.0	Falset	Tarragona	-2.26
07 November 1982	266.0	la Pobla de Lillet	Barcelona	-5.56
12 October 2016	257.0	Vilassar de Mar	Barcelona	-1.86
05 March 2013	253.5	Darnius	Girona	-5.32
29 November 2014	253.5	Parc Natural dels Ports	Tarragona	-4.54
16 February 1982	251.2	Amer	Girona	-2.41
25 September 1962	250.0	Martorelles	Barcelona	-1.52
04 November 1962	248.5	Sant Llorenç del Munt	Barcelona	-2.79
<i>02 September 1959</i>	<i>246.5</i>	<i>Cadaqués</i>	<i>Girona</i>	<i>-0.84</i>
10 October 1994	245.0	Beuda	Girona	-2.33
22 October 2000	240.0	Tivissa	Tarragona	-2.50
12 November 1999	233.5	Castellfollit de la Roca	Girona	-3.00
06 January 1977	233.0	Girona	Girona	-2.22
20 December 2007	230.2	Parc Natural dels Ports	Tarragona	-3.54
06 October 1959	230.1	Tossa de Mar	Girona	-1.36
03 October 1951	230.0	Cornellà de Llobregat	Barcelona	-1.02
20 September 1959	230.0	Gualba de Dalt	Barcelona	-1.49
11 October 1970	230.0	Riudabella	Tarragona	-1.61
23 October 2000	229.0	Horta de Sant Joan	Tarragona	-2.41
26 September 1992	226.4	Ampostà	Tarragona	-2.22
04 April 1969	226.0	Rupit	Barcelona	-2.21
12 November 1988	225.0	Corbera de Llobregat	Barcelona	-2.76
11 October 1962	223.0	Sils	Girona	-1.20
<i>20 November 1956</i>	<i>221.0</i>	<i>Cornellà de Llobregat</i>	<i>Barcelona</i>	<i>-0.45</i>
06 November 1983	220.0	Terrassa	Barcelona	-2.34
19 October 1994	220.0	el Port de Llançà	Girona	-2.36
<i>31 July 2002</i>	<i>218.2</i>	<i>Badalona</i>	<i>Barcelona</i>	<i>-0.13</i>
13 September 1963	217.5	l'Ametlla de Mar	Tarragona	-1.14
<i>19 September 1971</i>	<i>217.0</i>	<i>Xerta</i>	<i>Tarragona</i>	<i>-0.97</i>
<i>17 September 2010</i>	<i>216.8</i>	<i>l'Ametlla de Mar</i>	<i>Tarragona</i>	<i>-0.60</i>
17 October 2003	213.0	Vidrà	Girona	-2.48
<i>09 June 2000</i>	<i>210.0</i>	<i>el Bruc</i>	<i>Barcelona</i>	<i>-0.23</i>
<i>31 August 1975</i>	<i>208.5</i>	<i>Santa Agnès de Solius</i>	<i>Girona</i>	<i>-0.15</i>
29 January 1996	206.5	Fogars de Montclús	Barcelona	-2.37
<i>09 October 1971</i>	<i>204.0</i>	<i>Miravet</i>	<i>Tarragona</i>	<i>-0.86</i>
26 December 2008	202.5	Darnius	Girona	-2.84
07 May 2002	200.8	Godall	Tarragona	-2.47
07 October 1965	200.0	les Planes d'Hostoles	Girona	-2.12
27 October 1989	200.0	el Port de la Selva	Girona	-1.90
01 November 1993	200.0	Portbou	Girona	-2.57

233 Table 1. Catalogue of extreme torrential events (≥ 200 mm in 24 h, 7-7 UTC) in
234 Catalonia (NE Iberia) during the 1951-2016 period. Max RR is the highest
235 precipitation accumulation of the episode. The events are classified according to
236 the extreme negative Western Mediterranean Oscillation (WeMO) phase (bold),
237 the negative WeMO phase and the slight negative WeMO phase (italics).

238 3.2. Daily WeMOi values

239 The WeMOi is a regional teleconnection index defined within the Western
240 Mediterranean basin (Martin-Vide and Lopez-Bustins, 2006) and already used in
241 a wider range of studies (Azorin-Molina and Lopez-Bustins, 2008; Vicente-
242 Serrano *et al.*, 2009; Caloiero *et al.*, 2011; El Kenawy *et al.*, 2012; Coll *et al.*,
243 2014; Ríos-Cornejo *et al.*, 2015b; Lana *et al.*, 2017; Jghab *et al.*, 2019). WeMOi
244 values are computed by means of surface pressure data from the San Fernando
245 (SW Spain) and Padua (NE Italy) weather stations (Figure 3); the synoptic
246 window 30°-60°N - 15°W-20°E is found to best represent WeMO phases (Arbiol-
247 Roca *et al.*, 2018). Pressure data for both series were extracted from Martin-Vide
248 and Lopez-Bustins (2006), who performed a statistical treatment of
249 homogenization and the Climatology Group (University of Barcelona) periodically
250 update the data. The positive phase of the WeMO corresponds to the anticyclone
251 over the Azores encompassing the southwest quadrant of the Iberian Peninsula
252 and low pressures in the Gulf of Genoa (Figure 3a); its negative phase coincides
253 with an anticyclone located over Central or Eastern Europe and a low-pressure
254 centre, often cut off from the northern latitudes, within the framework of the
255 Iberian southwest (Figure 3b). Martin-Vide and Lopez-Bustins (2006) found that
256 the WeMOi was significantly and statistically correlated with precipitation over
257 areas that were weakly influenced by the North Atlantic Oscillation (NAO): these
258 areas are the northernmost and easternmost parts of Spain; precipitation over
259 the Cantabrian fringe (northern Spain) is strongly and positively correlated with
260 the WeMOi, and precipitation over the Spain's eastern façade is strongly and
261 negatively correlated with the WeMOi.

262

263

264

265

266

267

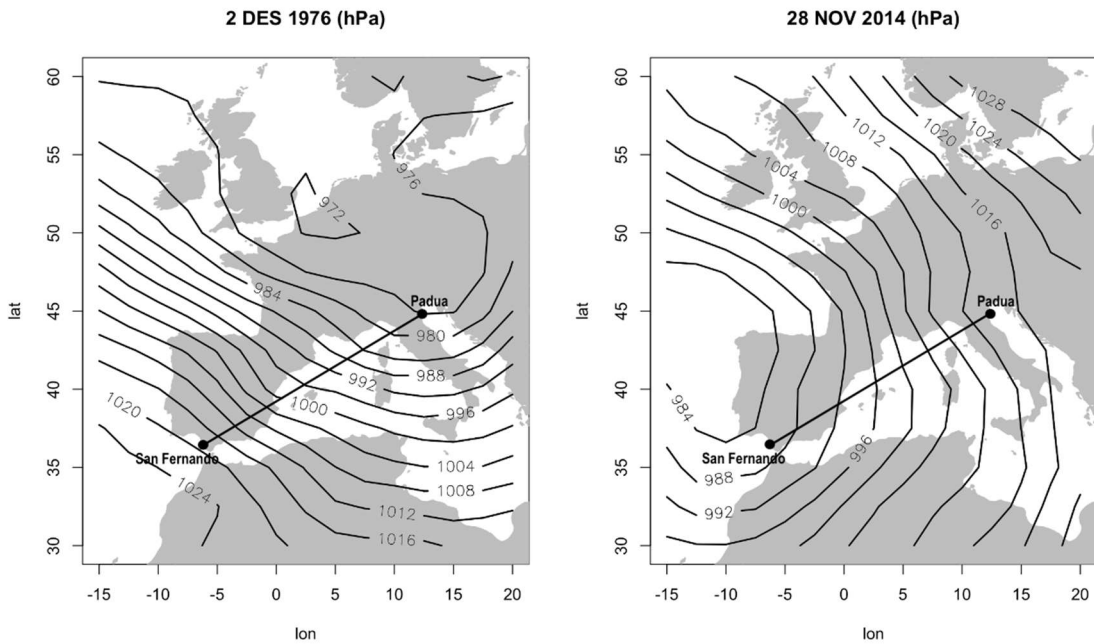
268

269

270

(a)

(b)



272

273 Figure 3. (a) Most extreme positive phase of the Western Mediterranean Oscillation
 274 (WeMO) in a daily synoptic situation during the 1951-2016 study period (2nd
 275 December 1976). (b) Most extreme negative WeMO phase in a daily synoptic situation
 276 during the 1951-2016 study period (28th November 2014). Data source: NCEP
 277 Reanalysis data provided by the NOAA/OAR/ESRL PSD, Boulder, Colorado, USA.

278 Application of the daily WeMOi is a methodological contribution by Martin-Vide
 279 and Lopez-Bustins (2006). It converts the low-frequency feature of the
 280 teleconnection patterns into a high-frequency mode. It is suitable for application
 281 both to the regional scale of the WeMO teleconnection pattern and the lesser
 282 variability of atmospheric pressure at Mediterranean latitudes. Patterns have
 283 rarely been used at daily resolution (Baldwin and Dunkerton, 2001; Beniston and
 284 Jungo, 2002; Azorin-Molina and Lopez-Bustins, 2008; Liu *et al.*, 2018). The
 285 method selected consists of previously standardizing each series of the dipole. It
 286 is necessary to use the daily mean and standard deviation of the 1961-1990
 287 reference period of all days of the year (January 1st 1961 – December 31st 1990).

288

289 For example, the WeMOi on January 1st 1981

290

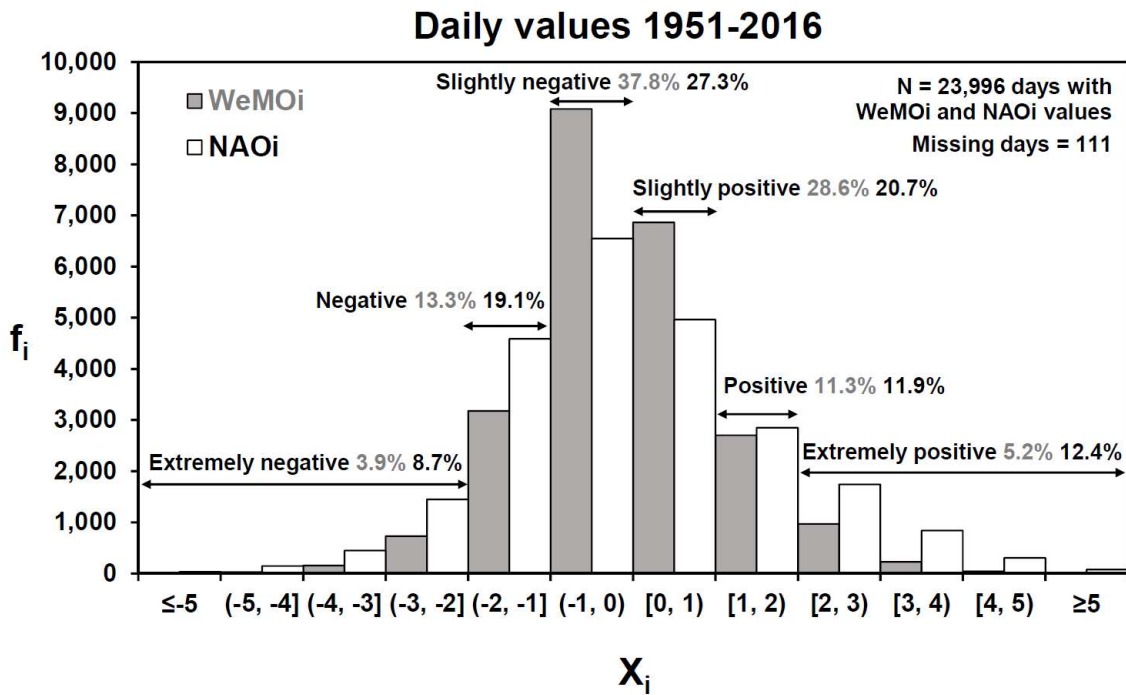
291
$$Z \text{ WeMOi Jan 1st 1981} = \frac{P \text{ Jan 1st 1981 SF} - \bar{X} \text{ 1961_1990 SF}}{S \text{ 1961_1990 SF}} - \frac{P \text{ Jan 1st 1981 PD} - \bar{X} \text{ 1961_1990 PD}}{S \text{ 1961_1990 PD}},$$

292 where P is pressure, SF, San Fernando, PD, Padua, \bar{X} , mean, and S, standard
293 deviation.

294

295 This calculation method, which considers all days of the year in the reference
296 period, enables all Mediterranean flows (negative WeMO phase) to be detected,
297 even if they are very weak. Otherwise, these moderate Mediterranean winds
298 would not be detected in autumn, since the WeMOi means are clearly negative
299 during this season. Likewise, the weak Mediterranean flows would be
300 overestimated in winter due to the high WeMOi mean during the coldest months.
301 According to previous studies (Martin-Vide and Lopez-Bustins, 2006; Azorin-
302 Molina and Lopez-Bustins, 2008), in the histogram of daily WeMOi frequencies,
303 WeMOi values between -1.00 and 1.00 are considered to constitute a neutral
304 WeMO phase, values ranging from 1.00 to 1.99 are considered as a positive
305 WeMO phase, those between -1.99 and -1.00 as a negative WeMO phase,
306 values ≥ 2.00 are deemed to represent an extreme positive WeMO phase and
307 those ≤ -2.00 to indicate an extreme negative WeMO phase. The most positive
308 WeMOi value (+5.99) of the 1951-2016 study period refers to December 2nd
309 1976 (Figure 3a), when an intense precipitation episode was recorded in the
310 Basque Country (northern Spain), according to ECA dataset (Klein Tank *et al.*,
311 2002; Cornes *et al.*, 2018). The most negative WeMOi value (-5.97) during the
312 1951-2016 period corresponds to November 28th 2014 (Figure 3b), when 253.5
313 mm was registered in the *Parc Natural dels Ports* (Tarragona) during the following
314 day (Table 1). Lana *et al.* (2016) studied the statistical complexity and
315 predictability of the WeMOi and demonstrated the Gaussian distribution of this
316 index. Most daily WeMOi values are negative (55%) and two thirds of the 23,996
317 days displaying WeMOi values correspond to a neutral WeMO phase (Figure 4).
318 The positive (negative) WeMO phase was detected in 16.5% (17.2%) of the total
319 days presenting a WeMOi value. The extreme WeMOi values, both positive
320 (5.2%) and negative (3.9%), represent less than 10% of the total number of days
321 for which WeMOi values are available. Daily NAO index (NAOi) values are also
322 used for comparison with WeMOi values and to enhance the role played by the
323 WeMO in torrential precipitation. Following the calculation method based on daily
324 WeMOi values, daily NAOi values are computed by means of surface pressure
325 data from the San Fernando (SW Spain) and Reykjavík (SW Iceland) weather

326 stations; the data for Reykjavík were provided by the ECA dataset (Klein Tank *et*
 327 *al.*, 2002). The NAOi values present the same percentage as that of the negative
 328 WeMOi daily values (55.1%) and almost half of the days are around 0. The
 329 distribution of the daily values of the NAOi presents more extreme positive and
 330 negative values than the WeMOi distribution, 12.4 vs 5.2% and 8.7 vs 3.9%,
 331 respectively (Figure 4).



332
 333 Figure 4. Frequency histogram of all daily WeMO index (WeMOi) values and
 334 North Atlantic Oscillation index (NAOi) values during the 1951-2016 study period.

335 3.3. Construction of calendars

336 Construction of calendars is a common procedure in climatological studies (Soler
 337 and Martin-Vide, 2002; Azorin-Molina and Lopez-Bustins, 2008; Meseguer-Ruiz
 338 *et al.*, 2018). They enable the intra-annual variability of the climate variable to be
 339 visualised. We computed daily WeMOi values for the 1951-2016 (66 years) study
 340 period, constructing two WeMOi calendars based upon the mean values obtained
 341 for each month, a 15-day period (i.e. a fortnight) and a 10-day period; the latter
 342 timescale corresponds approximately to the baroclinic prediction period (Holton,
 343 2004). The first climate calendar will show the annual cycle of the WeMOi values
 344 according to months (12 values), the second will display a more detailed intra-
 345 annual oscillation with 24 values and, finally, the 36 WeMOi values derived from
 346 the 10-day calendar will enable the slightest intra-annual variations in the WeMOi

347 to be detected. We will add to these calendars all the extreme torrential events in
348 order to observe correspondences between WeMOi values and heavy
349 precipitation events along the year. In order to detect any changes in the
350 calendars throughout the study period, we consider two subperiods for the
351 construction of two additional calendars: 1951-1983 (33 years) and 1984-2016
352 (33 years). We statistically tested the mean WeMOi values according to
353 subperiods in order to detect statistically significant differences. This statistical
354 significance is computed by means of a Normal distribution test according to
355 several confidence levels: 95.0% ($Z=1.960$), 99.0% ($Z=2.576$) and 99.9%
356 ($Z=3.291$).

357 Additionally, we analysed these calendars according to subperiods, together with
358 changes in SST and subsurface temperature at several depths (20, 50, and 80
359 m.b.s.l.) at a site located on the coast of Girona province (Figure 1). These data
360 constitute a reference series of sea temperature observations in Spain; the data
361 on the 1973-2017 period were provided by the Meteorological Service of
362 Catalonia. We calculated monthly temporal trends in sea temperatures using the
363 least-square linear fitting, and we estimated the statistical significance by means
364 of the Mann–Kendall non-parametric test (Sneyers, 1992). The standardized
365 values (Z) of sea temperatures were computed at 10-day resolution, and the Z
366 differences were obtained between two 5-yr subperiods from the beginning and
367 the end of the 1973-2017 period: 1973-1977 and 2013-2017; we showed the Z
368 differences for the months of the wet season (September, October and
369 November) for most of Catalonia (Figure 2b), and also for December in order to
370 detect a potential temporal shift of sea warming rates towards the early winter.

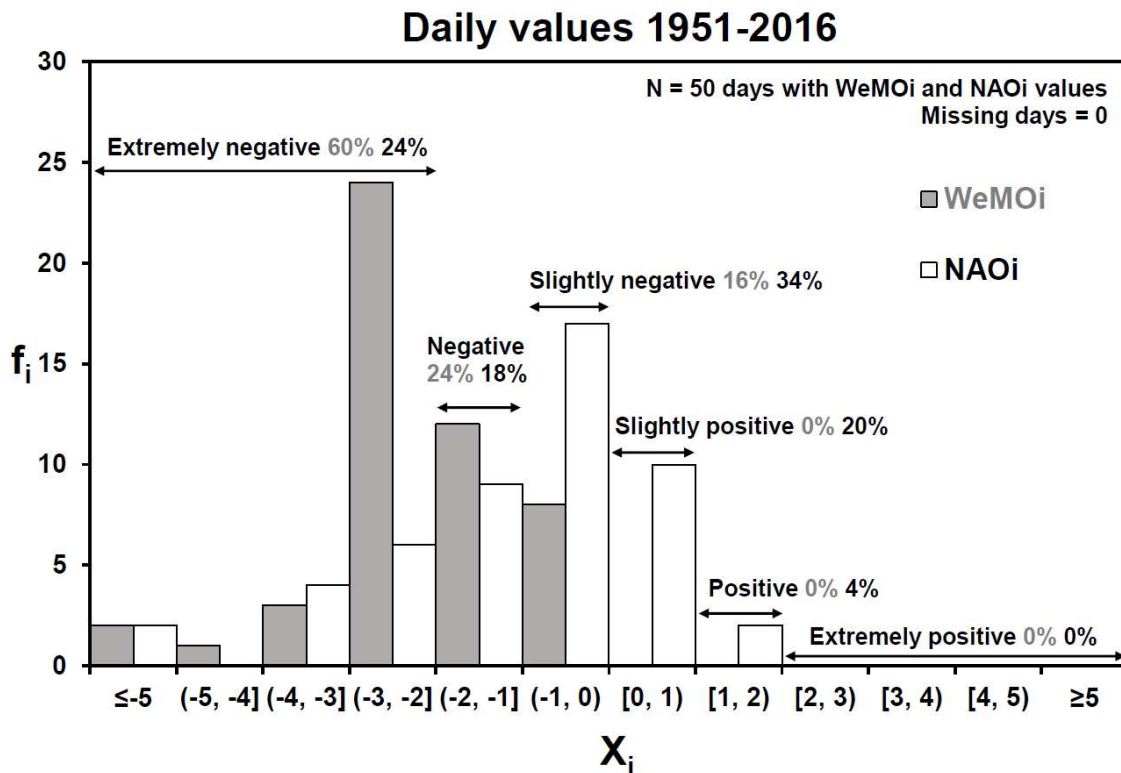
371 **4. Results and discussion**

372 *4.1. Frequency and temporal evolution of the extreme torrential events*

373 During the 1951-2016 period, 50 episodes presenting ≥ 200 mm in 24 h were
374 detected (0.8 cases per year) in Catalonia (Table 1); these were mainly
375 concentrated in the Eastern Pyrenees (Girona) and southern Catalonia
376 (Tarragona) (Figure 1). In the province of Lleida no maximum values for
377 precipitation episodes have been recorded, because this province is less
378 influenced by easterly flows as a result of its continental features. Other parts of

379 Iberia register a higher frequency of extreme torrential events, e.g. in the Valencia
380 Region, eastern Spain, there were 2 cases per year during the 1971-2000 period
381 (Riesco and Alcover, 2003). The highest frequency of torrential events (≥ 100 mm
382 in 24 h) over the Iberian Peninsula also corresponds to the Valencia Region,
383 where more than one case per year can be recorded by one same observatory
384 (Pérez-Cueva, 1994) and approximately 11 cases per year by all the stations in
385 the Valencia Region (Riesco and Alcover, 2003). Catalonia exhibits a lower
386 frequency of these torrential events (i.e. ≥ 100 mm in 24 h), 5-6 cases per year for
387 the whole region (Martin-Vide and Llasat, 2000; Lopez-Bustins *et al.*, 2016). The
388 highest precipitation amount during 7-7 UTC ever recorded in Catalonia is 430
389 mm. This occurred in Cadaqués (Cape Creus, in the easternmost part of the
390 Iberian Peninsula) on October 13th 1986. It was an extraordinary episode which
391 also affected the region of Pyrénées-Orientales (S France) (Vigneau, 1987),
392 albeit with a lower amount of precipitation than that produced by other extreme
393 torrential events of over 800 mm in Liguria Region (NW Italy), Valencia Region
394 (E Spain) and this region of Pyrénées-Orientales (Peñarrocha *et al.*, 2002).

395 Most of the episodes in Catalonia (60%) (30 events) took place in an extreme
396 negative (≤ -2.00) WeMO phase (Figure 5), whereas less than 4% of the total
397 number of days with WeMOi data showed a value equal to or lower than -2.00
398 (Figure 4). Moreover, 24% (12 events) of the episodes occurred in a negative (-
399 2.00, -1.00] WeMO phase. The remaining 8 events (16%) took place in a slightly
400 negative (-1.00, 0.00) WeMO phase. No extreme torrential episodes presenting
401 a positive WeMOi value occurred in Catalonia during the study period.
402 Furthermore, Martin-Vide and Lopez-Bustins (2006) found no positive daily
403 WeMOi values for torrential episodes (≥ 100 m in 24 h) in Tortosa (south
404 Catalonia) during the 1951-2000 period. On the other hand, the maximum
405 concentration of extreme torrential events according to NAOi values falls within
406 the interval (-1.00, 0.00), and both negative and positive NAOi values can account
407 for an event. This result demonstrates the fact that daily WeMOi values are more
408 useful than daily NAOi values. This is further evidenced by the fact that only 24%
409 of the total number of events took place during an extreme negative (≤ -2.00) NAO
410 phase, whereas this percentage rises to 60% in an extreme negative WeMO
411 phase.

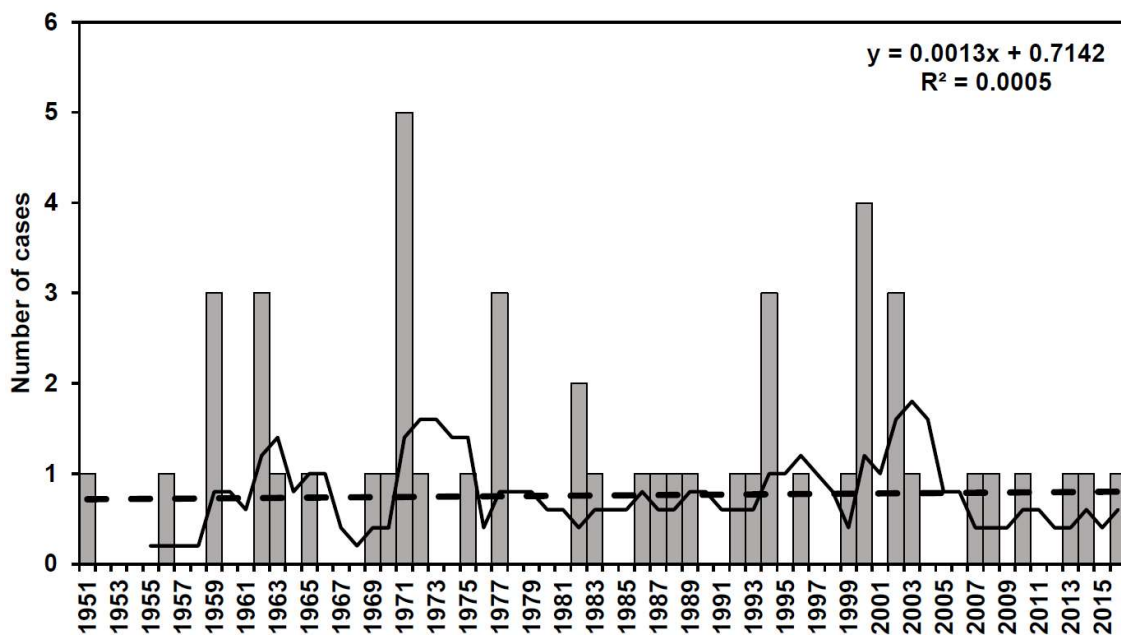


412

413 Figure 5. Frequency histogram of the daily WeMOi and NAOi values of the 50
414 extreme torrential events recorded in Catalonia during the 1951-2016 study period.

415 Most of the years in the 1951-2016 period present no episodes, or only one (Figure 6);
416 in six years there were 2 or 3 episodes, depending on the year, and in just two
417 years (1971 and 2000) we detected over 3 episodes in one year. The greatest
418 accumulation of cases can be observed in 1971, when a long-lasting torrential
419 episode exceeded the threshold of 200 mm in 24 h during four consecutive days
420 in September, with another one-day episode occurring in October. The former is
421 one of the most noteworthy episodes recorded in Catalonia (Llasat, 1990; Martin-
422 Vide and Llasat, 2000) in the last few decades. It started on September 19th in
423 southern Catalonia and ended on September 22nd in the northeast of the study
424 area (Llasat *et al.*, 2007). During the last decade, there has been no more than
425 one episode in one single year. However, for torrential events (≥ 100 mm in 24 h)
426 in Catalonia, Lopez-Bustins *et al.* (2016) detected a 45% increase in cases
427 between the 1950-1981 and 1982-2013 subperiods. In accordance with this rise
428 in torrential precipitation events, many studies on Iberian precipitation are
429 showing an increase in precipitation of Mediterranean origin in eastern Spain
430 (Miró *et al.*, 2009; Lopez-Bustins *et al.*, 2008; De Luis *et al.*, 2010); this

431 contributes to an increase in precipitation variability over the Western
 432 Mediterranean (Hartmann *et al.*, 2013, Caloiero *et al.*, 2019). On the other hand,
 433 non-statistical temporal trend is observed in the annual frequency of the extreme
 434 torrential episodes (i.e. ≥ 200 mm in 24 h) in Catalonia during the study period
 435 (Figure 6). This is in line with Llasat *et al.* (2016), who found non-statistical
 436 temporal trends in extreme daily precipitation in Catalonia.



437

438 Figure 6. Temporal evolution of the annual frequency of extreme torrential events
 439 (≥ 200 mm in 24 h) throughout the 1951-2016 study period. The figure shows the
 440 linear regression (dashed line) and 5-yr running mean (black line).

441 *4.2. Calendars of the daily WeMOi values*

442 The lowest WeMOi values are detected in autumn, especially in October (-0.38)
 443 (Figure 7a), usually with humid easterly flows from the Mediterranean Sea. This
 444 explains why autumn and October are the wettest season and month,
 445 respectively, on most of Spain's eastern façade (De Luis *et al.*, 2010). The
 446 greatest accumulation of extreme torrential events in Catalonia is in October, with
 447 19 events (38% of all cases). This is coherent with subsurface sea temperature,
 448 which reaches its annual maximum in autumn (not shown). September also
 449 shows a remarkable accumulation of events (11 cases), displaying the second
 450 lowest WeMOi monthly value (-0.29). Positive WeMOi values are observed from
 451 December to March, with very few events occurring. Sea temperature decreases

452 after the wet season, and the first months of the year constitute the period when
453 sea waters are the coldest (not shown). Additionally, WeMOi values are very high
454 in January and February, and the precipitation-convection phenomenon can
455 therefore be halted by a strong decrease in SST (Lebeaupin *et al.*, 2006).
456 Although negative WeMOi values are detected from April to November, very few
457 episodes are registered in late spring and summer; the predominance of
458 atmospheric stability during the warm season reduces the chances of extreme
459 torrential events occurring over the study area. At the fortnightly timescale, we
460 detected the minimum WeMOi value (-0.39) during the second half of October
461 (Figure 7b). The greatest accumulation of episodes, however, is in the first half
462 of October. The lowest WeMOi values are found from September 16th to October
463 31st. This short period of the year (46 days) accumulates over one half of the
464 total amount of extreme torrential events (28 cases, 56%). The most positive
465 WeMOi values are detected in the winter months, particularly from January 1st to
466 February 15th, and only 2 episodes are registered.

467 At the 10-day timescale, we observed the WeMOi minimum value (-0.45) from
468 October 11th to 20th (Figure 7c). This 10-day period also presents the largest
469 accumulation of extreme torrential events in Catalonia (8 cases; 16% of the total
470 number of cases). At least 4 cases are registered in each 10-day period from
471 September 11th to November 10th. This period of the year (61 days) accumulates
472 two thirds (33 cases, 66%) of all extreme torrential events. WeMOi values are
473 lower than -0.20 from August 1st to November 10th, fitting well with the period of
474 highest frequency of extreme torrential events in Catalonia. From August 1st to
475 September 10th, only 2 cases are registered due to the above-mentioned
476 atmospheric conditions in summer. From September 11th to November 10th,
477 favourable conditions can arise for the occurrence of extreme torrential events in
478 Catalonia: a high SST in the Western Mediterranean Sea and the early cut-off of
479 subpolar lows travelling to Mediterranean latitudes (Estrela *et al.*, 2008; Lopez-
480 Bustins, *et al.*, 2016; Pérez-Zanón *et al.*, 2018). The positive WeMOi values are
481 observed from December to March and each 10-day period presents either no
482 episode or only a single one. The most positive WeMOi value is observed from
483 January 1st to 10th (+0.38); this indicates the total predominance of the positive
484 phase of the teleconnection during these days, according to the 1951-2016 study

485 period (Figure 8a). During this 10-day period, the occurrence of extreme torrential
486 events in eastern Iberia is strongly inhibited by the NW atmospheric circulation
487 over the study area; sea waters are cold and the Genoa low is well represented.
488 The remaining 10-day periods in winter also present a predominance of the
489 western circulation over the Iberian Peninsula. This pattern causes positive
490 pressure differences between the Gulf of Cadiz (at a lower latitude) and the North
491 of Italy (at a higher latitude), which produces positive WeMOi values and inhibits
492 precipitation in eastern Iberia because of its location in the lee of the westerlies.
493 On the other hand, the mean sea level pressure (SLP) map from October 11th –
494 20th shows a predominance of the negative WeMO phase, with humid easterly
495 flows over Iberia, low pressure usually located in the Western Mediterranean
496 basin, and a blocking anticyclone over Central and Eastern Europe (Figure 8b).

497 This is approximately 60% of the year falling under negative WeMOi values at
498 monthly $N=8$ (out of 12) (Figure 7d), fortnightly $N=14$ (out of 24) (Figure 7e),
499 and 10-day $N=23$ (out of 36) (Figure 7f) timescales. The linear regression
500 between negative WeMOi values and episodes is statistically significant at all
501 timescales, providing an R of -0.73 (Figure 7d), -0.72 (Figure 7e) and -0.72
502 (Figure 7f). There is a statistically significant increase in the occurrence of events
503 as the WeMOi value decreases. The linear fitting is especially significant at 10-
504 day resolution.

505

506

507

508

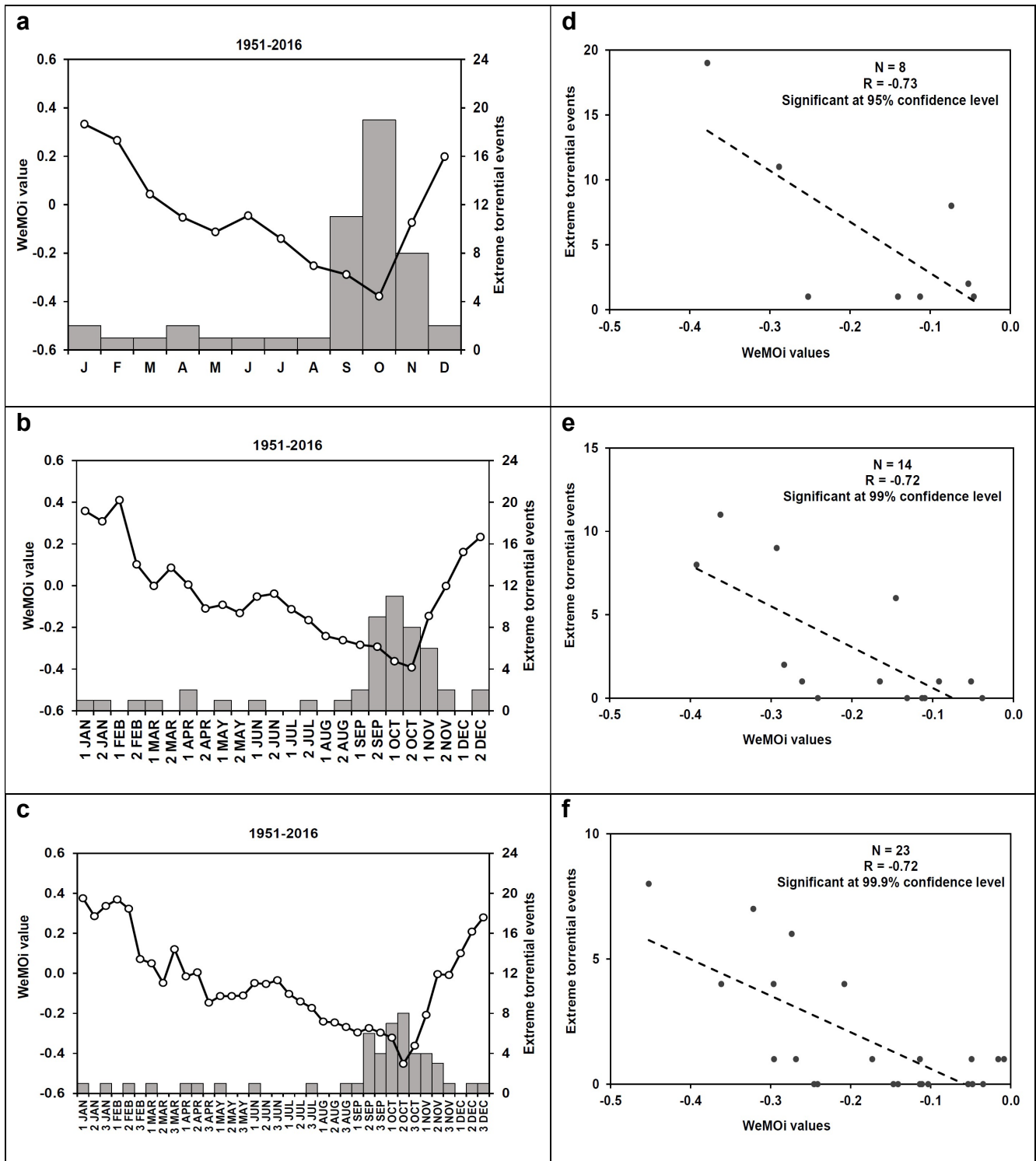
509

510

511

512

513

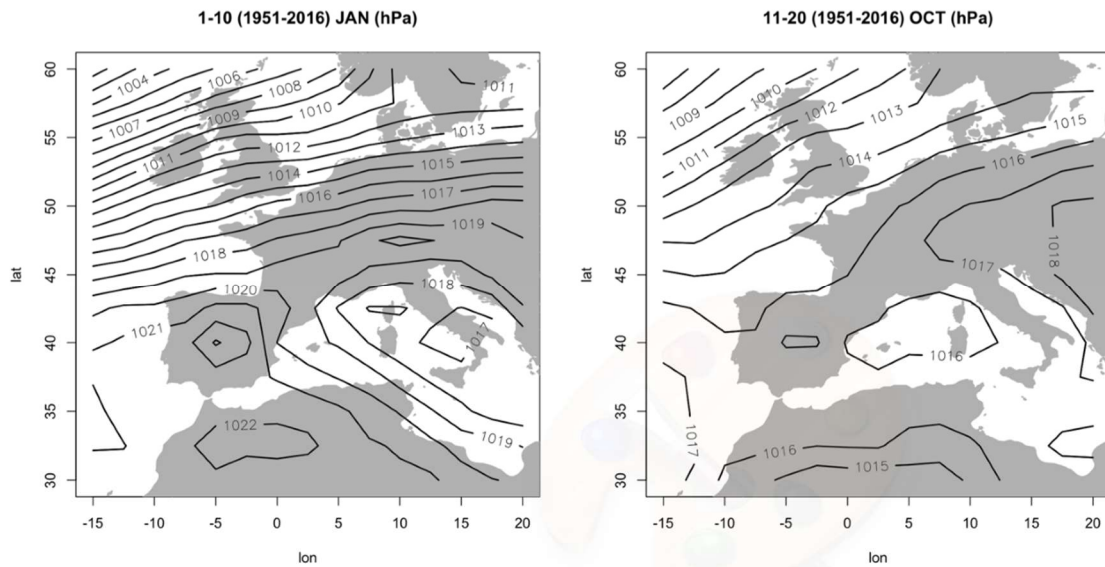


514 Figure 7. WeMOi calendars (lines) and frequency of extreme torrential episodes
 515 (bars) at several timescales: monthly (a), fortnightly (b) and 10-day (c).
 516 Scatterplot of the relationship between extreme torrential events and negative
 517 WeMOi values at several timescales: monthly (d), fortnightly (e) and 10-day (f);
 518 (the linear regression is shown as a dashed line).

520

(a)

(b)



521

522 Figure 8. Sea level pressure (SLP) mean of the synoptic window 30°N-60°N and
523 15°W-20°E from January 1st to 10th (a) and from October 11th to 20th (b) during
524 the 1951-2016 study period. Data source: NCEP Reanalysis data provided by the
525 NOAA/OAR/ESRL PSD, Boulder, Colorado, USA.

526 The WeMO teleconnection pattern can exert its influence upon precipitation
527 variability in other regions of Southern Europe (Caloiero *et al.*, 2011; Milosevic *et*
528 *al.*, 2016; Mathbout *et al.*, 2020). This central period of October may be the most
529 prone to torrential events over many regions of the western Mediterranean due
530 to presenting the lowest WeMOi value of the year. On the Iberian Peninsula, the
531 Almanzora river (SE Spain) suffered 2 of the 4 most catastrophic floods in the last
532 450 years within this central interval in October (Sánchez-García *et al.*, 2019).
533 Moreover, the deadliest torrential episodes in the Valencia Region (E Spain)
534 occurred on October 13th-14th 1957 and October 19th-20th 1982 (Olcina *et al.*,
535 2016; Miró *et al.*, 2017).

536

537 4.3. Subperiods and differences in the calendars

538 In relation to the calendars, and according to subperiods, we observed an overall
539 decrease in WeMOi values throughout the year (Figure 9). On the contrary, no
540 change was observed in the frequency of episodes between both subperiods;

541 exactly 25 extreme torrential events occurred in each subperiod. At the monthly
542 timescale, the extreme torrential period takes place in September and October
543 during the first half (1951-1983). For the second half (1984-2016), the maximum
544 accumulation of cases shifts from September-October to October-November,
545 with the highest concentration of cases in October, whilst new cases occur during
546 early winter (December). All WeMOi values are statistically and significantly lower
547 during the second subperiod than during the first one in all months, especially
548 from October to December. In the summer months, the decrease in WeMOi
549 values is moderate, albeit statistically significant due to the low variability of the
550 WeMOi values during the warm months. All these seasonal changes can be
551 related to trends in SST during the last few decades; the highest rate of SST
552 warming is in November (0.42 °C per decade) (Table 2). A general warming of
553 sea temperature has occurred along the year at all levels (SST, 20, 50, and 80
554 m.b.s.l.), particularly in spring, late autumn and early winter, a fact which might
555 explain these more negative WeMOi values during the second subperiod; the
556 warming of the lowest level of the atmosphere over the Western Mediterranean
557 Sea contributes to the formation of mesoscale lows (Jansà *et al.*, 2000). Similar
558 rates of warming at near-surface sea level have been recorded in other locations
559 in the north Mediterranean Sea (Raicich and Colucci, 2019). The highest warming
560 rates have been observed at SST and 20 m.b.s.l., but the statistical significance
561 has been greater at the deepest levels, i.e. 50 and 80 m.b.s.l. (Table 2). Figure
562 10 shows that changes in WeMOi values between both subperiods are negatively
563 and statistically correlated with sea temperature trends, above all, in the
564 underlying layers, especially at 80 m.b.s.l., where sea temperature displays a low
565 interannual and intra-annual variability and sea heat content hardly varies
566 (Sparnocchia *et al.*, 2006).

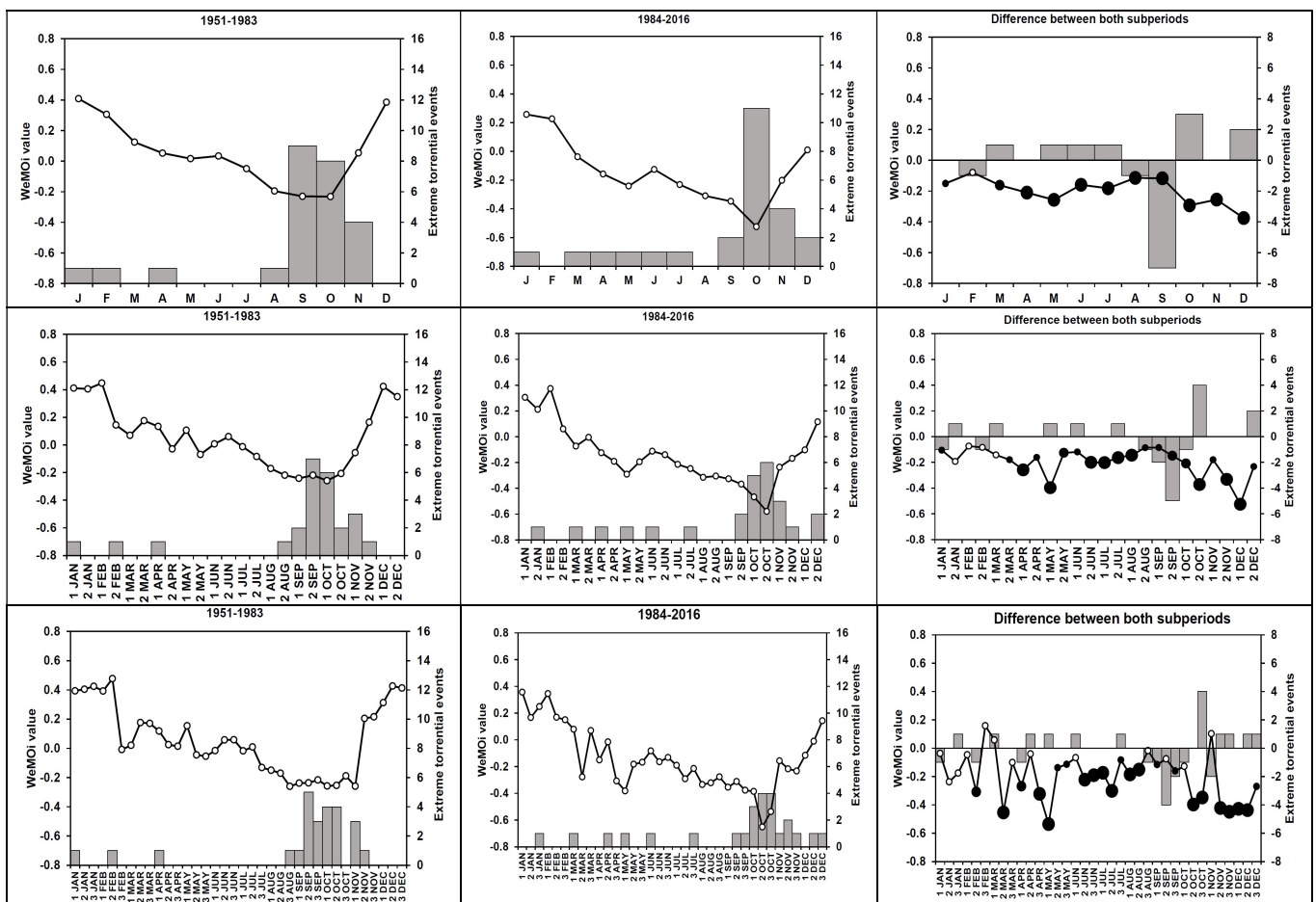
567 At the fortnightly timescale, a shifting of maximum torrentiality is observed from
568 September 16th – October 15th to October 1st – October 31st. The lowest WeMOi
569 value of the calendar from 1951 to 1983 was in the first fortnight of October (-
570 0.26); however, the lowest value is observed in the second fortnight of October
571 during the 1984-2016 period (-0.58). All WeMOi values according to fortnights
572 showed a statistical and significant decrease during the second period, except
573 from January 16th to March 15th. The sharpest decline in WeMOi values is in the

574 first fortnight of May, the second fortnight of October, the second fortnight of
575 November and the first fortnight of December. The lowest WeMOi value during
576 the second subperiod is detected in the second fortnight of October, when the
577 greatest increase in extreme torrential events is observed.

578 At the 10-day timescale the lowest WeMOi values remain relatively constant from
579 the end of August to the beginning of November during the first subperiod, which
580 corresponds well with the occurrence of extreme torrential events. During the second
581 subperiod, the lowest WeMOi values are found from October 11th to 31st, with an
582 accumulation of 8 cases (32% of the total number of cases of the second subperiod).
583 A continuous and statistically significant decrease in WeMOi values (at the 99.9%
584 confidence level) is observed from October 16th to December 20th during the
585 second subperiod, except for the first 10-day period of November. The increase in
586 torrential events is especially concentrated from October 21st to 31st. From August
587 21st to October 10th there is an overall decline in extreme torrential events, which
588 might be associated with the fact that the WeMOi values hardly show a decrease
589 over these 10-day periods of the year during the second subperiod. This is in line
590 with the fact that the warming was moderate, or that there was even a certain degree
591 of cooling, during the first 10-day periods of the wet season, i.e. from September 1st
592 to October 20th, in the underlying sea layers (Table 3); and consequently, episodes
593 might not have been favoured during the second subperiod. The highest sea
594 temperature increase at all levels during the wet season is in the third 10-day period
595 of October (Table 3), when the highest increase in extreme torrential episodes is
596 observed (Figure 9). The changes in the frequency of episodes are statistically
597 correlated with sea temperatures at subsurface layers, i.e. 50 and 80 m.b.s.l. (Figure
598 11). The deepest level (80 m.b.s.l.) shows the strongest warming in late autumn
599 (from October 21st to November 30th), whereas this warming is weak in early
600 autumn (from September 1st to October 20th) (Figure 12).

601 In general terms, no more cases of extreme torrential events are observed during
602 the 1984-2016 period in comparison with the 1951-1983 period. Nonetheless, a
603 greater accumulation of cases can be observed during late autumn and a lesser
604 accumulation in early autumn during the second subperiod, in comparison with the
605 first one. A sharp and continuous drop in WeMOi values is observed at the very end
606 of autumn, which might indicate a shift in the seasonality of the extreme torrential

607 period from September-October to October-November and an increase in
 608 precipitation irregularity due to a deeper WeMO negative phase (Lopez-Bustins and
 609 Lemus-Canovas, 2020). This seasonal shifting might be caused by a recent increase
 610 in sea temperature in the Western Mediterranean basin, particularly in November
 611 (Table 2) and late October (Table 3) (Lopez-Bustins, 2007; Estrela *et al.*, 2008;
 612 Lopez-Bustins *et al.*, 2016; Arbiol-Roca *et al.*, 2017). Pastor *et al.* (2018) used
 613 satellite data to identify an overall increase in SST throughout the Mediterranean
 614 basin during the 1982-2016 period, highlighting its role in torrential events in the
 615 Western Mediterranean.

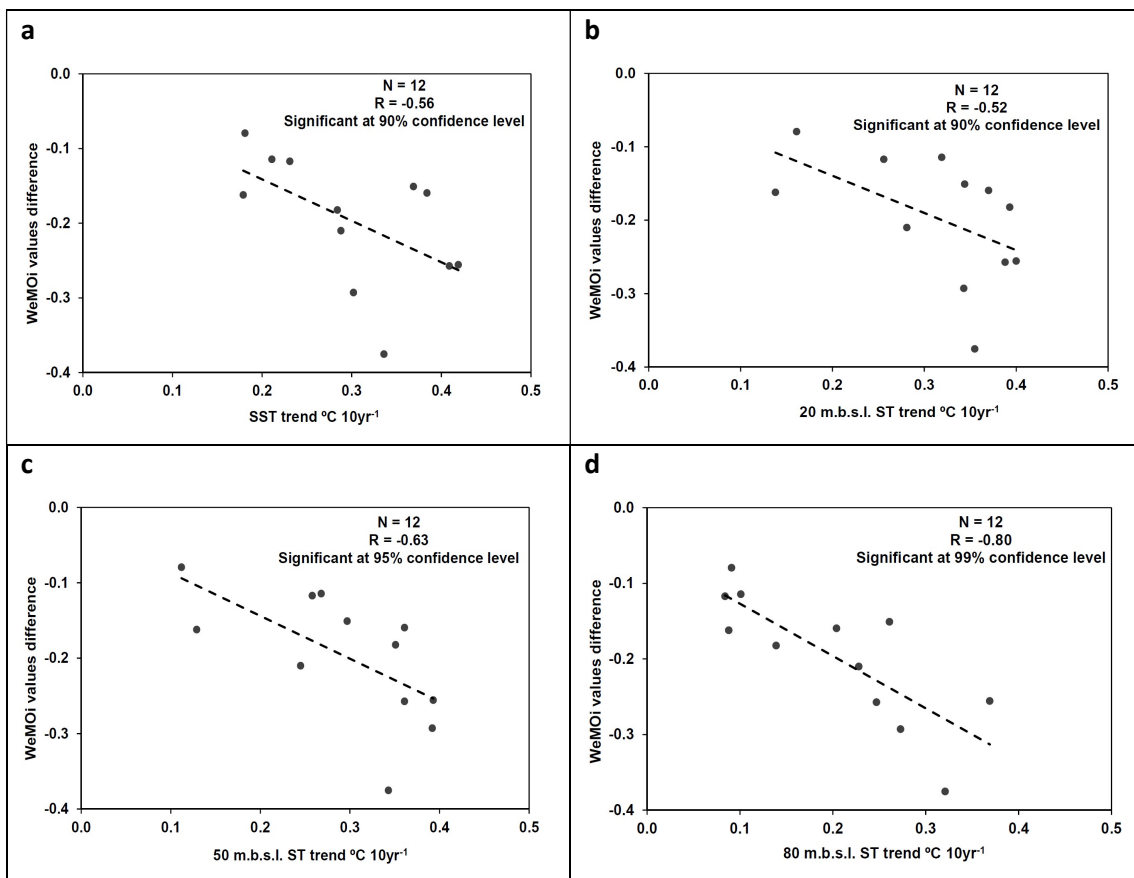


616 Figure 9. WeMOi calendars (lines) and frequency of extreme torrential episodes (bars)
 617 at several timescales: monthly (above), fortnightly (middle) and 10-day (below) for the
 618 1951-1983 (left) and 1984-2016 (central) subperiods. The right-hand column shows
 619 the difference in the number of episodes and WeMOi values between both subperiods
 620 (for WeMOi values: white dots indicate not statistically significant differences, and
 621 small-, medium- and large-sized black dots show statistically significant differences
 622 at the 95.0%, 99.0% and 99.9% confidence levels, respectively).

N = 44 1973-2016		J	F	M	A	M	J	J	A	S	O	N	D	°C 10yr ⁻¹	
SST	*	*	*	*	*	*	*	*	*	*	*	*	*	<0.15	0.30-0.34
-20 m	*	*		*	*	*	*	*	*	*	*	*	*	0.15-0.19	0.35-0.39
-50 m	*			*	*	*	*	*	*	*	*	*	*	0.20-0.24	≥0.40
-80 m	*			*	*	*	*	*	*	*	*	*	*	0.25-0.29	

623 Table 2. Monthly sea temperature trends at surface (SST), 20, 50, and 80 m.b.s.l.
 624 during 1973-2016 (*statistically significant trends at the 95% confidence level by
 625 means of the Mann-Kendall non-parametric test).

626



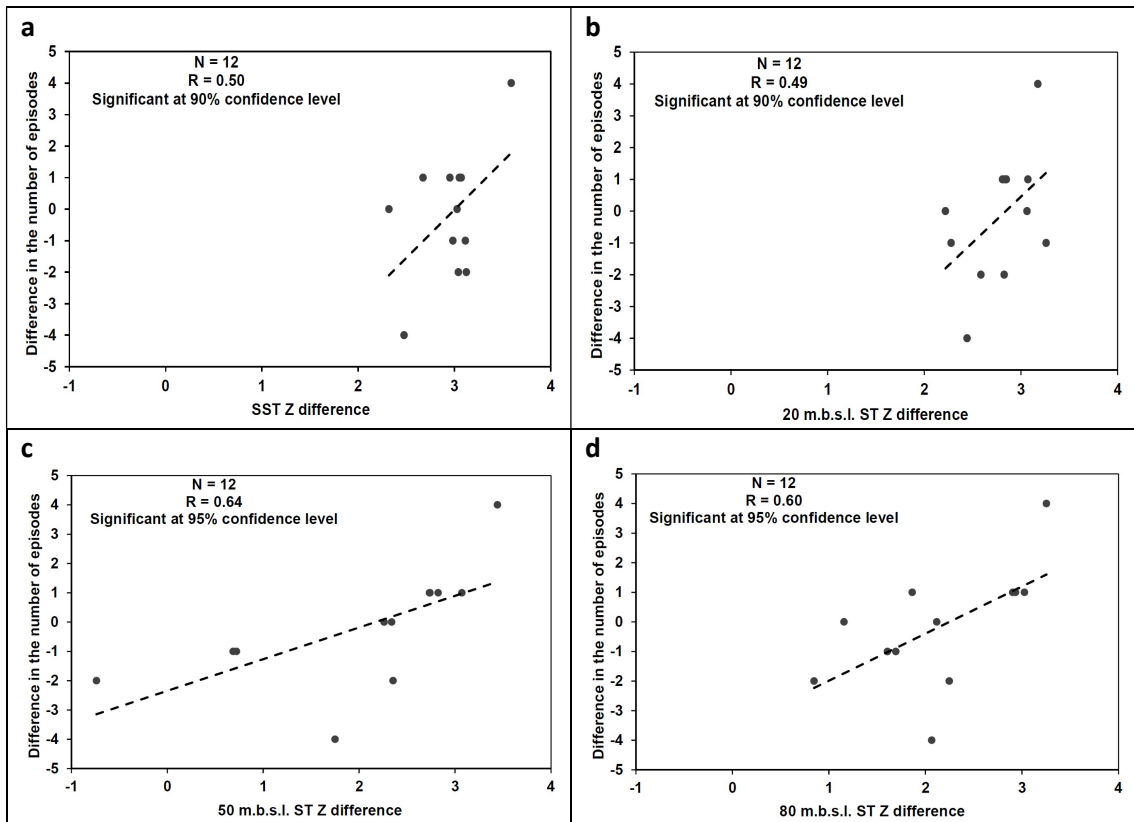
627 Figure 10. Scatterplot of the monthly relationship between the WeMOi value
 628 differences (1984-2016 minus 1951-1983) and sea temperature (ST) trends
 629 during the 1973-2016 period at surface (SST) (a), 20 (b), 50 (c), and 80 (d)
 630 m.b.s.l. (a dashed line indicates the linear regression).

631
 632
 633
 634
 635
 636

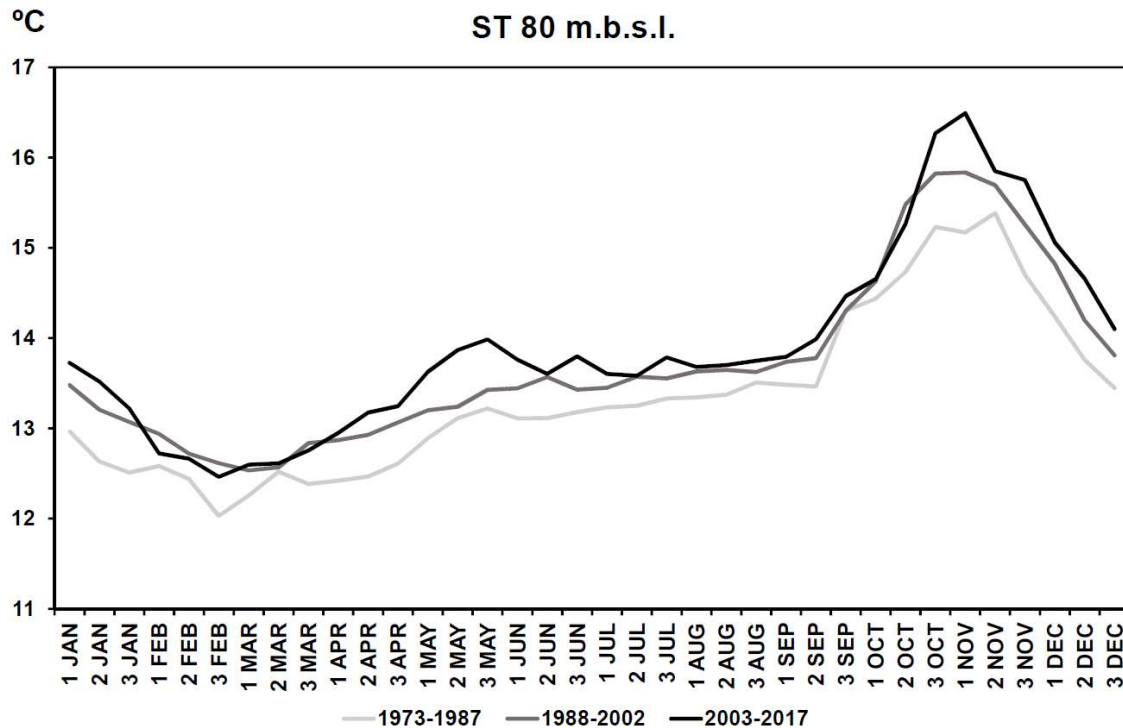
	1	2	3	1	2	3	1	2	3	1	2	3	Z	
	SEP	SEP	SEP	OCT	OCT	OCT	NOV	NOV	NOV	DEC	DEC	DEC	<0.00	
SST													0.00-0.49	2.00-2.49
-20 m													0.50-0.99	2.50-2.99
-50 m													1.00-1.49	3.00-3.49
-80 m													1.50-1.99	≥3.50

637 Table 3. 10-day period ST standardized values (Z) differences for two 5-yr
638 subperiods (2013-2017 minus 1973-1977) at surface, 20, 50, and 80 m.b.s.l.
639 during the wet season (from September to November) and December.

640



641 Figure 11. Scatterplot of the 10-day relationship between the differences in the
642 number of episodes (1984-2016 minus 1951-1983) and ST Z differences for two
643 5-yr subperiods (2013-2017 minus 1973-1977) at surface (a), 20 (b), 50 (c), and
644 80 (d) m.b.s.l. during the wet season (from September to November) and
645 December (a dashed line indicates the linear regression).



646

647 Figure 12. ST 10-day calendar at 80 m.b.s.l. for three 15-yr subperiods: 1973-
 648 1987, 1988-2002 and 2003-2017.

649 **5. Conclusions**

650 The present research confirms the usefulness of the WeMOi at daily resolution
 651 as an effective tool for analysing the occurrence of episodes of torrential
 652 precipitation over NE Spain. October is the rainiest month in most regions of the
 653 Northwestern Mediterranean basin and can account for the lowest value of the
 654 year on the WeMOi monthly calendar, together with the warmest sea temperature
 655 of the year at subsurface level. Moreover, most torrential episodes take place
 656 during a very short period in the middle of this month.

657 Catalonia is located in the Northwestern Mediterranean basin and its extreme
 658 precipitation is highly dependent upon the atmospheric circulation over the
 659 Mediterranean. The present study considers the threshold of 200 mm in 24 h for
 660 extreme torrential episodes, due to the fact that this precipitation accumulation in
 661 one day can cause serious widespread damage over a large area. Having
 662 thoroughly reviewed several databases and contrasted these results with the
 663 original files and nearby weather stations, we confirmed that Catalonia registered

664 0.8 cases per year (50 episodes in 66 years) of extreme torrential episodes during
665 the 1951-2016 study period, in accordance with the 7-7 UTC pluviometric day.

666 The 10-day period from October 11th to 20th exhibits both the greatest
667 accumulation of extreme torrential episodes in Catalonia and the lowest intra-
668 annual WeMOi value. This 10-day period has been demonstrated to be the most
669 prone to torrential events in this Northwestern Mediterranean area, according to
670 the WeMOi values. The most intense torrential event in Catalonia ever recorded
671 by an official weather station is in Cape Creus (the easternmost part of the Iberian
672 Peninsula) within the 10-day period most susceptible to torrential precipitation
673 (October 13th 1986), with a total amount of 430 mm. The most positive WeMO
674 phase of the year usually takes place in January, especially from January 1st to
675 10th, when the synoptic and sea temperature conditions of this time of the year
676 inhibit torrential events.

677 No extreme torrential episodes in Catalonia occurred in a positive WeMO phase.
678 Additionally, 60% of the cases occurred in an extreme negative WeMO phase,
679 i.e. a WeMOi value equal to or lower than -2.00. In the present study this threshold
680 is considered to constitute the onset of a rainstorm favoured by a strong
681 Mediterranean flow. The lower WeMOi value is related to an increase in extreme
682 torrential events at all timescales. On comparing both study subperiods (1951-
683 1983 and 1984-2016), an overall statistically significant decrease is detected in
684 most WeMOi values of the year, especially at the end of October and some
685 periods in November and December. This might have been caused by an overall
686 increase in sea temperature throughout the year, particularly in late autumn. On
687 the other hand, extreme torrential events show no changes in frequency between
688 both subperiods; no temporal trend is observed, either, during the 1951-2016
689 study period. The most notable change involves the displacement of extreme
690 torrential episodes from early to late autumn; this is in accordance with the lower
691 WeMOi values detected in the last three months of the year during the second
692 subperiod. Increases in sea temperatures in the underlying layers during the end
693 of the wet season can provide an understanding of these changes in extreme
694 torrential events and in the WeMOi calendars.

695

696 **Data availability**

697 The WeMOi data can be downloaded from the Climatology Group (University of
698 Barcelona) website <http://www.ub.edu/gc/en/> (last accessed May 23rd 2020).

699 **Author contributions**

700 JALB performed the analysis and wrote the paper. LAR updated the WeMOi data
701 and plotted the pressure maps. JMV discussed the results. ABE elaborated the
702 inventory of the episodes and discussed the results. MPD discussed the results.

703 **Competing interests**

704 The authors declare that they have no conflict of interest.

705 **Acknowledgments**

706 The present study was conducted within the framework of the Climatology Group
707 of the University of Barcelona (2017 SGR 1362, Catalan Government) and the
708 CLICES Spanish project (CGL2017-83866-C3-2-R). Our research benefited from
709 the daily precipitation data provided by the Meteorological Service of Catalonia.
710 We are especially indebted to the meteorological observer from l'Estartit (Girona
711 province), Josep Pascual, who painstakingly recorded sea temperature data over
712 the last few decades.

713 **References**

714 Alfieri, L., Burek, P., Feyen, L., Forzieri, G., 2015. Global warming increases the
715 frequency of river floods in Europe. *Hydrology and Earth System Sciences* 19,
716 2247-2260. DOI: 10.5194/hess-19-2247-2015, 2015.

717 Arbiol-Roca, L., Lopez-Bustins, J.A., Martin-Vide, J.: The role of the WeMOi in
718 the occurrence of torrential rainfall in Catalonia (NE Iberia). Abstracts book: 6th
719 International Conference on Meteorology and Climatology of the Mediterranean
720 (MetMed). Zagreb (Croatia): ACAM, 2017.

721 Arbiol-Roca, L., Lopez-Bustins, J.A., Esteban-Vea, P., Martin-Vide, J.: Cálculo
722 del índice de la Oscilación del Mediterráneo Occidental con técnicas de análisis
723 multivariante. In: Montávez-Gómez, J.P., Gómez-Navarro, J.J., López-Romero,
724 J.M., Palacios-Peña, L., Turco, M., Jerez-Rodríguez, S., Lorente, R., Jiménez-

725 Guerrero, P. (eds.), *El Clima: Aire, Agua, Tierra y Fuego*, pp. 761-771. Cartagena
726 (Spain): Asociación Española de Climatología (AEC), 2018.

727 Armengot, R.: *Las lluvias intensas en la Comunidad Valenciana*. 263 pp. Madrid
728 (Spain): Ministerio de Medio Ambiente, Dirección General del Instituto Nacional
729 de Meteorología, 2002.

730 Azorin-Molina, C., Lopez-Bustins, J.A.: An automated sea breeze selection
731 based on regional sea-level pressure difference: WeMOi. *International Journal of*
732 *Climatology* 28, 1681-1692. DOI: 10.1002/joc.1663, 2008.

733 Baldwin, M.P., Dunkerton T.J.: Stratospheric harbingers of anomalous weather
734 regimes. *Science* 294, 581-584. DOI: 10.1126/science.1063315, 2001.

735 Barrera-Escoda, A., Gonçalves, M., Guerreiro, D., Cunillera, J., Baldasano, J.M.:
736 Projections of temperature and precipitation extremes in the North Western
737 Mediterranean Basin by dynamical downscaling of climate scenarios at high
738 resolution (1971-2050). *Climate Change* 122, 567-582. DOI: 10.1007/s10584-
739 013-1027-6, 2014.

740 Beguería, S., Angulo-Martínez, M., Vicente-Serrano, S.M., López-Moreno, J.I.,
741 Kenawy, A.: Assessing trends in extreme precipitation events intensity and
742 magnitude using non-stationary peaks-over-threshold analysis: a case study in
743 northeast Spain from 1930 to 2006. *International Journal of Climatology* 31, 2102-
744 2114. DOI:10.1002/joc.2218, 2011.

745 Beniston, M., Junco, P.: Shifts in the distributions of pressure, temperature and
746 moisture in the Alpine region in response to the behaviour of the North Atlantic
747 Oscillation. *Theoretical and Applied Climatology* 71, 29-42. DOI: 10.1007/s704-
748 002-8206-7, 2002.

749 Caloiero, T., Coscarelli, R., Ferrari, E., Mancini, M.: Precipitation change in
750 Southern Italy linked to global scale oscillation indexes. *Natural Hazards and*
751 *Earth System Sciences* 11, 1683-1694. DOI: 10.5194/nhess-11-1683-2011,
752 2011.

753 Caloiero, T., Coscarelli, R., Gaudio, R.: Spatial and temporal variability of daily
754 precipitation concentration in the Sardinia region (Italy). *International Journal of*
755 *Climatology* 39, 5006–5021, 2019.

756 Christensen, J.H., K. Krishna Kumar, E. Aldrian, S.-I. An, I.F.A. Cavalcanti, M. de
757 Castro, W. Dong, P. Goswami, A. Hall, J.K. Kanyanga, A. Kitoh, J. Kossin, N.-C.
758 Lau, J. Renwick, D.B. Stephenson, S.-P. Xie and T. Zhou, T.: Climate
759 Phenomena and their Relevance for Future Regional Climate Change. In:
760 Climate Change 2013: The Physical Science Basis. Contribution of Working
761 Group I to the Fifth Assessment Report of the Intergovernmental Panel on
762 Climate Change [Stocker, T.F., D. Qin, G.-K. Plattner, M. Tignor, S.K. Allen, J.
763 Boschung, A. Nauels, Y. Xia, V. Bex and P.M. Midgley (eds.)]. Cambridge
764 University Press, Cambridge, United Kingdom and New York, NY, USA. DOI:
765 10.1017/CBO9781107415324.028, 2013.

766 Coll, M., Carreras, M., Ciércoles, C., Cornax, M.J., Gorelli, G., Morote, E., Sáez,
767 R.: Assessing fishing and marine biodiversity changes using fishers' perceptions:
768 the Spanish Mediterranean and Gulf of Cadiz case study. PLoS ONE 9(1):
769 e85670. DOI: 10.1371/journal.pone.0085670, 2014.

770 Cornes, R., van der Schrier, G., van den Besselaar, E.J.M., Jones, P.D.: An
771 Ensemble Version of the E-OBS Temperature and Precipitation Datasets.
772 Journal of Geophysical Research: Atmospheres 123, 9391-9409. DOI:
773 10.1029/2017JD028200, 2018.

774 Cortesi, N., Gonzalez-Hidalgo, J.C., Brunetti, M., Martin-Vide, J.: Daily
775 precipitation concentration across Europe 1971-2010. Natural Hazards and Earth
776 System Sciences 12, 2799-2810. DOI: 10.5194/nhess-12-2799-2012, 2012.

777 Cramer, W., Guiot, J., Fader, M., Garrabou, J., Gattuso, J.P., Iglesias, A., Lange,
778 M.A., Lionello, P., Llasat, M.C., Paz, S., Peñuelas, J., Snoussi, M., Toreti, A.,
779 Tsimplis, M.N., Xoplaki, E.: Climate change and interconnected risks to
780 sustainable development in the Mediterranean. Nature Climate Change 8, 972–
781 DOI: 10.1038/s41558-018-0299-2, 2018.

782 De Luis, M., Brunetti, M., Gonzalez-Hidalgo, J.C., Longares, L.A., Martin-Vide, J.:
783 Changes in seasonal precipitation in the Iberian Peninsula during 1946-2005.
784 Global and Planetary Change 74, 27-33. DOI: 10.1038/s41558-018-0299-2,
785 2010.

786 El Kenawy, A., López-Moreno, J.I., Vicente-Serrano, S.M.: Trend and variability
787 of surface air temperature in northeastern Spain (1920-2006): Linkage to
788 atmospheric circulation. *Atmospheric Research* 106, 159-180. DOI:
789 10.1016/j.atmosres.2011.12.006, 2012.

790 Estrela, M.J., Pastor, F., Miró, J., Valiente, J.A.: Precipitaciones torrenciales en
791 la Comunidad Valenciana: La temperatura superficial del agua del mar y áreas
792 de recarga. Primeros resultados. In: M.J. Estrela Navarro (ed.), *Riesgos
793 climáticos y cambio global en el mediterráneo español ¿hacia un clima de
794 extremos?*, pp. 121-140. Valencia (Spain): Colección Interciencias, 2008.

795 Gil-Guirado, S., Pérez-Morales, A., Lopez-Martinez, F.: SMC-Flood database: a
796 high-resolution press database on flood cases for the Spanish Mediterranean
797 coast (1960–2015). *Natural Hazards and Earth System Sciences* 19, 1955-1971.
798 DOI: 10.5194/nhess-19-1955-2019, 2019.

799 Gilabert, J., Llasat, M.C.: Circulation weather types associated with extreme flood
800 events in Northwestern Mediterranean. *International Journal of Climatology*, 38,
801 1864-1876. DOI:10.1002/joc.5301, 2018.

802 González-Hidalgo, J.C., Lopez-Bustins, J.A., Stepanek, P. Martin-Vide, J., De
803 Luis, M.: Monthly precipitation trends on the Mediterranean fringe of the Iberian
804 Peninsula during the second-half of the twentieth century (1951-2000).
805 *International Journal of Climatology* 29, 415-1429. DOI: 10.1002/joc.1780, 2009.

806 González-Hidalgo, J. C., Brunetti, M., de Luis, M.: A new tool for monthly
807 precipitation analysis in Spain: MOPREDAS database (monthly precipitation
808 trends December 1945–November 2005). *International Journal of Climatology*
809 31, 715-731. DOI: 10.1002/joc.2115, 2011.

810 Greve, P., Gudmundsson, L., Seneviratne, S.I.: Regional scaling of annual mean
811 precipitation and water availability with global temperature change. *Earth System
812 Dynamics Discussion* 9, 227-240. DOI: 10.3929/ethz-b-000251688, 2018.

813 Holton, J.R.: *An Introduction to Dynamic Meteorology*. Elsevier Academic Press,
814 *International Geophysics Series*, volume 88, 4th edition, 535 pp, 2004.

815 Hartmann, D.L., Klein Tank, A.M.G., Rusticucci, M., Alexander, L.V.,
816 Brönnimann, S., Charabi, Y., Dentener, F.J., Dlugokencky, E.J., Easterling, D.R.,

817 Kaplan, A., Soden, B.J., Thorne, P.W., Wild, M., Zhai, P.M.: Observations:
818 Atmosphere and Surface. In: Climate Change 2013: The Physical Science Basis.
819 Contribution of Working Group I to the Fifth Assessment Report of the
820 Intergovernmental Panel on Climate Change [Stocker, T.F., D. Qin, G.-K.
821 Plattner, M. Tignor, S.K. Allen, J. Boschung, A. Nauels, Y. Xia, V. Bex and P.M.
822 Midgley (eds.)]. Cambridge University Press, Cambridge, United Kingdom and
823 New York, NY, USA. DOI: 10.1017/CBO9781107415324.008, 2013.

824 Iizuka, S., Nakamura, H.: Sensitivity of midlatitude heavy precipitation to SST: A
825 case study in the Sea of Japan area on 9 August 2013. *Journal of Geophysical*
826 *Research: Atmospheres*, 124, 4365–4381. DOI:10.1029/2018JD029503, 2019.

827 Jang, J.H.: An advanced method to apply multiple rainfall thresholds for urban
828 flood warnings. *Water* 7, 6056-6078. DOI: 10.3390/w7116056, 2015.

829 Jansà, A., Genovés, A.: Western Mediterranean cyclones and heavy rain. Part 1:
830 Numerical experiment concerning the Piedmont flood case. *Meteorological*
831 *Applications*, 7(4), 323-333. DOI:10.1017/S1350482700001663, 2000.

832 Jansà, A., Genovés, A., Riosalido, R., Carretero, O.: Mesoscale cyclones vs
833 heavy rain and MCS in the Western Mediterranean. *MAP newsletter*, 5, 24-25,
834 1996.

835 Jansà, A., Genovés, A., Picornell, M., Campins, J., Riosalido, R., Carretero, O.:
836 Western Mediterranean cyclones and heavy rain. Part 2: Statistical approach.
837 *Meteorological Applications*, 8(1), 43-56. DOI:10.1017/S1350482701001049,
838 2000.

839 Jghab, A., Vargas-Yañez, M., Reul, A., Garcia-Martínez, M.C., Hidalgo, M.,
840 Moya, F., Bernal, M., Ben Omar, M., Benchoucha, S., Lamtai, A.: The influence
841 of environmental factors and hydrodynamics on sardine (*Sardina pilchardus*,
842 Walbaum 1792) abundance in the southern Alboran Sea. *Journal of Marine*
843 *Systems* 191, 51-63. DOI: 10.1016/j.jmarsys.2018.12.002, 2019.

844 Klein Tank, A.M.G., Wijngaard, J.B., Können, G.P., Böhm, R., Demarée, G.,
845 Gocheva, A., Mileta, M., Pashiardis, S., Hejkrlik, L., Kern-Hansen, C., Heino, R.,
846 Bessemoulin, P., Müller-Westermeier, G., Tzanakou, M., Szalai, S., Pálsdóttir,
847 T., Fitzgerald, D., Rubin, S., Capaldo, M., Maugeri, M., Leitass, A., Bukatis,

848 A., Aberfeld, R., van Engelen, A.F.V., Forland, E., Mietus, M., Coelho, F., Mares,
849 C., Razuvaev, V., Nieplova, E., Cegnar, T., López, J.A., Dahlström, B., Moberg,
850 A., Kirchhofer, W., Ceylan, A., Pachaliuk, O., Alexander, L.V., Petrovic, P.: Daily
851 dataset of 20th-century surface air temperature and precipitation series for the
852 European climate assessment. *International Journal of Climatology* 22, 1441-
853 1453. DOI: 10.1002/joc.773, 2002.

854 Knoben, W.J.M., Woods, R.A., Freer, J.E.: Global bimodal precipitation
855 seasonality: A systematic overview. *International Journal of Climatology* 39, 558
856 - 567. DOI: 10.1002/joc.5786, 2019.

857 Kottek, M., Grieser, J., Beck, C., Rudolf, B., Rubel, F.: World Map of the Köppen-
858 Geiger climate classification updated. *Meteorologische Zeitschrift* 15, 259-263.
859 DOI: 10.1127/0941-2948/2006/0130, 2006.

860 Kreibich, H., Di Baldassarre, G., Vorogushyn, S., Aerts, J.C.J.H., Apel, H.,
861 Aronica, G.T., Arnbjerg-Nielsen, K., Bouwer, L.M., Bubeck, P., Caloiero, T.,
862 Chinh, D.T., Cortès, M. Gain, A.K., Giampá, V., Kuhlicke, C., Kundzewicz, Z.W.,
863 Llasat, M.C., Mård, J., Matczak, P., Mazzoleni, M., Molinari, D., Dung, N.V.,
864 Petrucci, O., Schröter, K., Slager, K., Thielen, A.H., Ward, P.J., Merz, B.:
865 Adaptation to flood risk: Results of international paired flood event studies.
866 *Earth's Future* 5, 953-965. DOI: 10.1002/2017EF000606, 2017.

867 Lana, X., Burgueño, A., Martínez, M.D., Serra, C.: Complexity and predictability
868 of the monthly Western Mediterranean Oscillation index. *International Journal of*
869 *Climatology* 36, 2435-2450. DOI: 10.1002/joc.4503, 2016.

870 Lana, X., Burgueño, A., Martínez, M.D., Serra, C.: Monthly rain amounts at Fabra
871 Observatory (Barcelona, NE Spain): fractal structure, autoregressive processes
872 and correlation with monthly Western Mediterranean Oscillation index.
873 *International Journal of Climatology* 37, 1557-1577. DOI: 10.1002/joc.4797,
874 2017.

875 Lebeaupin, C., Ducrocq, V., Giordani, H. Sensitivity of Mediterranean torrential
876 rain events to the sea surface temperature based on high-resolution numerical
877 forecasts. *Journal of Geophysical Research* 111, D12110.
878 doi:10.1029/2005JD006541, 2006.

879 Liu, Y.; Li, Z.; Yin, H.: A timely El Niño-Southern Oscillation forecast method
880 based on daily Niño index to ensure food security. Published in: 2018 7th
881 International Conference on Agro-geoinformatics (Agro-geoinformatics) DOI:
882 10.1109/Agro-Geoinformatics.2018.8476070, 2018.

883 Llasat, M.C.: Influencia de la orografía y de la inestabilidad convectiva en la
884 distribución espacial de lluvias extremas en Cataluña. *Acta Geologica Hispanica*
885 25, 197-208, 1990.

886 Llasat, M.C.: High magnitude storms and floods, in Woodward, J.C. (ed.). *The*
887 *Physical Geography of the Mediterranean*. Oxford University Press, Oxford, UK,
888 513-540, 2009.

889 Llasat, M.C., Martín, F., Barrera, A.: From the concept of 'kaltlufttropfen' (cold air
890 pool) to the cut-off low. The case of September 1971 in Spain as an example of
891 their role in heavy rainfalls. *Meteorology and Atmospheric Physics* 96, 43-60.
892 DOI: 10.1007/s00703-006-0220-9, 2007.

893 Llasat, M.C., Marcos, R., Turco, M., Gilabert, J., Llasat-Botija, M.: Trends in flash
894 flood events versus convective precipitation in the Mediterranean region: The
895 case of Catalonia. *Journal of Hydrology* 541, 24-37. DOI:
896 10.1016/j.jhydrol.2016.05.040, 2016.

897 Lopez-Bustins, J.A.: *The Western Mediterranean Oscillation and Rainfall in the*
898 *Catalan Countries*. PhD Thesis, Department of Physical Geography and Regional
899 Geographical Analysis, University of Barcelona, 184 pp, 2007.

900 Lopez-Bustins, J.A.: Lluvias fuertes, pero mal repartidas. El caso del clima
901 mediterráneo. *Biblio3W Revista Bibliográfica de Geografía y Ciencias Sociales*
902 vol. 23, no 1243, 2018.

903 Lopez-Bustins, J.A., Lemus-Canovas, M.: The influence of the Western
904 Mediterranean Oscillation upon the spatiotemporal variability of precipitation over
905 Catalonia (northeastern of the Iberian Peninsula). *Atmospheric Research* 236,
906 104819, DOI: 10.1016/j.atmosres.2019.104819, 2020.

907 Lopez-Bustins, J.A., Martin-Vide, J., Sanchez-Lorenzo, A.: Iberia winter rainfall
908 trends based upon changes in teleconnection and circulation patterns. *Global*

909 and Planetary Change 63, 171-176. DOI: 10.1016/j.gloplacha.2007.09.002,
910 2008.

911 Lopez-Bustins, J.A., Martin-Vide, J., Prohom, M., Cordobilla, M.J.: Variabilidad
912 intraanual de la Oscilación del Mediterráneo Occidental (WeMO) y ocurrencia de
913 episodios torrenciales en Cataluña. In: Olcina, J., Rico, A.M., Moltó, E. (eds.),
914 Clima, sociedad, riesgos y ordenación del territorio, pp. 171-182. Alicante
915 (Spain): Asociación Española de Climatología (AEC), 2016.

916 Martin-Vide, J.: Aplicación de la clasificación sinóptica automática de Jenkinson
917 y Collison a días de precipitación torrencial en el este de España. In: Cuadrat,
918 J.M., Vicente-Serrano, S., Saz, M.A. (eds.), La información climática como
919 herramienta de gestión ambiental, pp. 123-127, Zaragoza (Spain): University of
920 Zaragoza, 2002.

921 Martin-Vide, J., Llasat, M.C.: Las precipitaciones torrenciales en Cataluña. Serie
922 Geográfica 9, 17-26, 2000.

923 Martin-Vide, J., Lopez-Bustins, J.A.: The Western Mediterranean Oscillation and
924 rainfall in the Iberian Peninsula. International Journal of Climatology 26, 1455-
925 1475. DOI: 10.1002/joc.1388, 2006.

926 Martin-Vide, J., Raso-Nadal, J.M.: Atlas Climàtic de Catalunya, 1961-1990. 32
927 pp. Barcelona (Spain): Servei Meteorològic de Catalunya, Departament de Medi
928 Ambient i Habitatge, Generalitat de Catalunya, 2008.

929 Martin-Vide, J.P., Llasat, M.C.: The 1962 flash flood in the Rubí stream
930 (Barcelona, Spain). Journal of Hydrology 566, 441-454. DOI:
931 10.1016/j.jhydrol.2018.09.028, 2018.

932 Martin-Vide, J., Sanchez-Lorenzo, A., Lopez-Bustins, J.A., Cordobilla, M.J.,
933 Garcia-Manuel, A., Raso, J.M.: Torrential rainfall in northeast of the Iberian
934 Peninsula: synoptic patterns and WeMO influence. Advances in Science and
935 Research 2, 99-105. DOI: 10.5194/asr-2-99-2008, 2008.

936 Martina, M.L.V., Todini, E., Libralon, A.: Rainfall thresholds for flood warning
937 systems: a Bayesian decision approach. In: Sorooshian S., Hsu KL., Coppola E.,
938 Tomassetti B., Verdecchia M., Visconti G. (eds.), Hydrological Modelling and the
939 Water Cycle. Water Science and Technology Library, vol 63, pp. 203-227.

940 Springer, Berlin, Heidelberg (Germany). DOI: 10.1007/978-3-540-77843-1_9,
941 2009.

942 Mathbout, S., Lopez-Bustins, J.A., Royé, D., Martin-Vide, J., Benhamrouche, A.:
943 Spatiotemporal variability of daily precipitation concentration and its relationship
944 to teleconnection patterns over the Mediterranean during 1975-2015.
945 International Journal of Climatology 40, 1435-1455. DOI: 10.1002/joc.6278,
946 2020.

947 Merino, M., Fernández-Vaquero, M., López, L., Fernández-González, S.,
948 Hermida, L., Sánchez, J.L., García-Ortega, E., Gascón, E.: Large-scale patterns
949 of daily precipitation extremes on the Iberian Peninsula. International Journal of
950 Climatology 36, 3873-3891. DOI: 10.1002/joc.4601, 2016.

951 Meseguer-Ruiz, O., Lopez-Bustins, J.A., Arbiol-Roca, L., Martin-Vide, J., Miró, J.,
952 Estrela, M.J.: Episodios de precipitación torrencial en el este y sureste ibéricos y
953 su relación con la variabilidad intraanual de la Oscilación del Mediterráneo
954 Occidental (WeMO) entre 1950 y 2016. In: Montávez-Gómez, J.P., Gómez-
955 Navarro, J.J., López-Romero, J.M., Palacios-Peña, L., Turco, M., Jerez-
956 Rodríguez, S., Lorente, R., Jiménez-Guerrero, P. (eds.), El Clima: Aire, Agua,
957 Tierra y Fuego, pp. 53-63. Cartagena (Spain): Asociación Española de
958 Climatología (AEC), 2018.

959 Milosevic, D.D., Savic, S.M., Pantelic, M., Stankov, U., Ziberna, I., Dolinaj, D.,
960 Lescesen, I.: Variability of seasonal and annual precipitation in Slovenia and its
961 correlation with large-scale atmospheric circulation. Open Geosciences 8, 593-
962 605. DOI: 10.1515/geo-2016-0041, 2016.

963 Miró, J., Estrela, M.J., Pastor, F., Millán, M.: Análisis comparativo de tendencias
964 en la precipitación, por distintos inputs, entre los dominios hidrológicos del
965 Segura y del Júcar (1958-2008). Investigaciones Geográficas 49, 129-157, 2009.

966 Miró, J.J., Caselles, V., Estrela, M.J.: Multiple imputation of rainfall missing data
967 in the Iberian Mediterranean context. Atmospheric Research 197, 313-330. DOI:
968 10.1016/j.atmosres.2017.07.016, 2017.

969 Nakamura, I., Llasat, M.C.: Policy and systems of flood risk management: a
970 comparative study between Japan and Spain. *Natural Hazards* 87, 919-943. DOI:
971 10.1007/s11069-017-2802-x, 2017.

972 Naranjo-Fernández, N., Guardiola-Albert, C., Aguilera, H., Serrano-Hidalgo, C.,
973 Rodríguez-Rodríguez, M., Fernández-Ayuso, A., Ruiz-Bermudo, F., Montero-
974 González, E.: Relevance of spatio-temporal rainfall variability regarding
975 groundwater management challenges under global change: case study in
976 Doñana (SW Spain). *Stochastic Environmental Research and Risk Assessment*,
977 DOI:10.1007/s00477-020-01771-7, 2020.

978 Norbiato, D., Borga, M., Esposti, S.D., Gaume, e., Anquetin, S.: Flash flood
979 warning based on rainfall thresholds and soil moisture conditions: An assessment
980 for gauged and ungauged basins. *Journal of Hydrology* 362, 274-290. DOI:
981 10.1016/j.jhydrol.2008.08.023, 2008.

982 Olcina, J., Sauri, D., Hernández, M., Ribas, A.: Flood policy in Spain: a review for
983 the period 1983-2013. *Disaster Prevention and Management* 25, 41-58. DOI:
984 10.1108/DPM-05-2015-0108, 2016.

985 Papalexiou, S.M., Montanari, A.: Global and regional increase of precipitation
986 extremes under global warming. *Water Resources Research* 55, 4901-4914.
987 DOI: 10.1029/2018WR024067, 2019.

988 Pastor, F., Valiente, J. A., Estrela, M. J.: Sea surface temperature and torrential
989 rains in the Valencia region: modelling the role of recharge areas. *Natural*
990 *Hazards and Earth System Sciences* 15, 1677-1693, 2015.

991 Pastor, F., Valiente, J.A., Palau, J.L.: Sea Surface Temperature in the
992 Mediterranean: Trends and Spatial Patterns (1982–2016). *Pure and Applied*
993 *Geophysics* 175, 4017–4029. DOI:10.1007/s00024-017-1739-z, 2018.

994 Peña, J.C., Aran, M., Pérez-Zanón, N., Casas-Castillo, M.C., Rodríguez-Solà, R.,
995 Redaño, A.: Análisis de las situaciones sinópticas correspondientes a episodios
996 de lluvia severa en Barcelona. In: *Libro de Resúmenes de la XXXV Reunión*
997 *Bienal de la Real Sociedad Española de Física*, pp. 450-451. Gijón (Spain): Real
998 *Sociedad Española de Física (RSEF)*, 2015.

999 Peñarrocha, D., Estrela, M.J., Millán, M.: Classification of daily rainfall patterns in
1000 a Mediterranean area with extreme intensity levels: the Valencia region.
1001 International Journal of Climatology 22, 677-695. DOI: 10.1002/joc.747, 2002.

1002 Pérez-Cueva, A.J.: Atlas Climàtic de la Comunitat Valenciana (1961-1990), 205
1003 pp. Valencia (Spain): Generalitat Valenciana, 1994.

1004 Pérez-Zanón, N., Casas-Castillo, M.C., Peña, J.C., Aran, M., Rodríguez-Solà, R.,
1005 Redaño, A., Solé, G.: Analysis of synoptic patterns in relationship with severe
1006 rainfall events in the Ebre Observatory (Catalonia). Acta Geophysica 66, 405-
1007 414. DOI: 10.1007/s11600-018-0126-1, 2018.

1008 Raicich, F., Colucci, R.R.: A near-surface sea temperature time series from
1009 Trieste, northern Adriatic Sea (1899-2015). Earth System Science Data 11, 2,
1010 761-768, 2019.

1011 Riesco, J., Alcover, V.: Predicción de precipitaciones intensas de origen marítimo
1012 mediterráneo en la Comunidad Valenciana y la Región de Murcia. 124 pp. Madrid
1013 (Spain): Centro de Publicaciones, Secretaría General Técnica, Ministerio de
1014 Medio Ambiente, 2003.

1015 Rigo, T., Llasat, M.C.: Features of convective systems in the NW of the
1016 Mediterranean Sea. Proceedings of the 5th EGU Plinius Conference on
1017 Mediterranean Storms 1-2 October 2003, Ajaccio, France. European
1018 Geosciences Union, pp. 73-79, 2003.

1019 Ríos-Cornejo, D., Penas, A., Álvarez-Esteban, R., del Río, S.: Links between
1020 teleconnection patterns and precipitation in Spain. Atmospheric Research 156,
1021 14-28. DOI: 10.1016/j.atmosres.2014.12.012, 2015a.

1022 Ríos-Cornejo, D., Penas, A., Álvarez-Esteban, R., del Río, S.: Links between
1023 teleconnection patterns and mean temperature in Spain. Theoretical and Applied
1024 Climatology 122, 1-18. DOI: 10.1007/s00704-014-1256-2, 2015b.

1025 Rodó, X., Baert, E., Comin, F.A.: Variations in seasonal rainfall in Southern
1026 Europe during the present century: relationships with the North Atlantic
1027 Oscillation and the El Niño-Southern Oscillation. Climate Dynamics 13, 275-284,
1028 1997.

1029 Rodríguez-Puebla, C., Encinas, A.H., Sáenz, J.: Winter precipitation over the
1030 Iberian Peninsula and its relationship to circulation indices. *Hydrology and Earth*
1031 *System Sciences* 5, 233-244, 2001.

1032 Romero, R., Sumner, G., Ramis, C., Genovés, A.: A classification of the
1033 atmospheric circulation patterns producing significant daily rainfall in the Spanish
1034 Mediterranean area. *International Journal of Climatology* 19, 765-789, 1999.

1035 Sánchez-García, C., Schulte, L., Carvalho, F., Peña, J.C.: A 500-year flood
1036 history of the arid environments of southeastern Spain. The case of the
1037 Almanzora River. *Global and Planetary Change* 181, DOI:
1038 10.1016/j.gloplacha.2019.102987, 2019.

1039 SMC-Servei Meteorològic de Catalunya: Yearly Bulletin of Climate Indicators,
1040 2016. Technical report. Meteorological Service of Catalonia, Department of
1041 Territory and Sustainability, Government of Catalonia, Barcelona, 88 pp.
1042 Available at: [https://static-m.meteo.cat/wordpressweb/wp-](https://static-m.meteo.cat/wordpressweb/wp-content/uploads/2017/05/29072030/00_BAIC-2016_TOT.pdf)
1043 [content/uploads/2017/05/29072030/00_BAIC-2016_TOT.pdf](https://static-m.meteo.cat/wordpressweb/wp-content/uploads/2017/05/29072030/00_BAIC-2016_TOT.pdf). Climate monthly
1044 series available at: [https://www.meteo.cat/wpweb/climatologia/serveis-i-dades-](https://www.meteo.cat/wpweb/climatologia/serveis-i-dades-climatiques/series-climatiques-historiques/)
1045 [climatiques/series-climatiques-historiques/](https://www.meteo.cat/wpweb/climatologia/serveis-i-dades-climatiques/series-climatiques-historiques/), 2017.

1046 Sneyers, R.: On the use of statistical analysis for the objective determination of
1047 climate change. *Meteorologische Zeitschrift* 1, 247–256, 1992.

1048 Soler, X., Martin-Vide, J.: Los calendarios climáticos. Una propuesta
1049 metodológica. In: Guijarro, J.A., Grimalt, M., Laita, M., Alonso, S. (eds.), *El Agua*
1050 *y el Clima*, pp. 577-586. Mallorca (Spain): Asociación Española de Climatología,
1051 2002.

1052 Sparnocchia, S., Schiano, M.E., Picco, P., Bozzano, R., Cappelletti, A.: The
1053 anomalous warming of summer 2003 in the surface layer of the Central Ligurian
1054 Sea (Western Mediterranean). *Annales Geophysicae* 24, 2, 443-452, 2006.

1055 Trigo, R.M., Pozo-Vázquez, D., Osborn, T.J., Castro-Díez, Y., Gámiz-Fortis, S.,
1056 Esteban-Parra, M.J.: North Atlantic Oscillation influence on precipitation, river
1057 flow and water resources in the Iberian Peninsula. *International Journal of*
1058 *Climatology* 24, 925-944. DOI: 10.1002/joc.1048, 2004.

1059 Vicente-Serrano, S.M., Beguería, S., López-Moreno, J.I., El Kenawy, A.M.,
1060 Angulo-Martínez, M.: Daily atmospheric circulation events and extreme
1061 precipitation risk in northeast Spain: Role of the North Atlantic Oscillation, the
1062 Western Mediterranean Oscillation, and the Mediterranean Oscillation. *Journal of*
1063 *Geophysical Research* 114, D08106. DOI: 10.1029/2008JD011492, 2009.

1064 Vigneau, J.-P.: 1986 dans les Pyrénées Orientales: deux perturbations
1065 méditerranéennes aux effets remarquables. *Revue Géographique des Pyrénées*
1066 *et du Sud-Ouest* 58, 23-54. DOI:10.3406/rgpso.1987.4969, 1987.

1067 Wergen, D., Volovik, D., Redner, S., Krug, J.: Rounding Effects in Record
1068 Statistics. *Physical Review Letters* 109(16): 164102. DOI:
1069 10.1103/PhysRevLett.109.164102, 2012.